Lukas Heupl, BSc

Ion Uptake of Blended Polymer Resins

MASTERARBEIT

Zur Erlangung des akademischen Grades

Diplom-Ingenieur

Masterprogramm Technische Chemie

Eingereicht an der

Technischen Universität Graz

Institute for Chemistry and Technology of Materials

Betreuer:

Priv.-Doz. Dipl.-Chem.Univ. Dr.rer.nat. Frank Wiesbrock

Graz, Dezember 2018

EIDESSTATTLICHE ERKLÄRUNG

Ich erkläre an Eides statt, dass ich die vorliegende Arbeit selbstständig verfasst, andere als die angegebenen Quellen/Hilfsmittel nicht benutzt, und die den benutzten Quellen wörtlich und inhaltlich entnommenen Stellen als solche kenntlich gemacht habe. Das in TUGRAZonline hochgeladene Textdokument ist mit der vorliegenden Masterarbeit identisch.

Datum

Unterschrift

STATUTORY DECLARATION

I declare that I have authored this thesis independently, that I have not used other than the declared sources / resources, and that I have explicitly marked all material which has been quoted either literally or by content from the used sources.

date

signature

Acknowledgement

This research work was performed within the K-Project 'PolyTherm' at the Polymer Competence Center Leoben GmbH (PCCL) within the framework of the COMET-program of the Federal Ministry for Transport, Innovation and Technology and the Federal Ministry of Digital and Economic Affairs with contributions by the Graz University of Technology and the Montanuniversitaet Leoben. Funding is provided by the Austrian Government and the State Government of Styria.

In the first place I want to thank my supervisor Priv.-Doz. Dipl.-Chem.Univ. Dr.rer.nat. Frank Wiesbrock for the great support throughout the whole work. Due to his professional advice and help in many situations, I was able to gain a lot of knowledge within the research topic and was able to realize this work.

Especially, I want to thank Josefine Hobisch for performing the GPC measurements and thermal analyses, Petra Kaschnitz for the assistance with NMR measurements, and Helmar Wiltsche for the performance of the ICP-OES analyses. SEM-EDX and impedance measurements were performed with equipment of the VARTA Micro Innovation GmbH; Bernd Fuchsbichler and Christoph Stangl are acknowledged for their kind support.

Of course, I want to thank all my friends and fellow students, especially Sarah Rendl, Wolfgang Fortmüller, Hannes Kühnle, Josef Lechner, Rene Nauschnig, Ulrike Reisinger, Elisabeth Rossegger, Werner Schlemmer, Bettina Schweda, Jakob Strasser and Lara Strohmeier.

Many thanks go to my colleagues of the working group, Inge Mühlbacher, Sarah Rendl, Robin Hofmann, Philipp Marx and Matthias Windberger for having a great time, as well to the colleagues from the whole institute, especially Birgit Ehmann for her constant support.

Inhalt

1. Introduction

The developments in the semiconductor industry rapidly advance and, therefore, the requirements for different components and materials constantly grow. In 1965, Moore predicted that the number of transistors on a circuit board would double each year [1]. As a matter of fact, his hypothesis is still valid, even after more than 50 years.

Due to the reduction of the size of transistors, many challenges have arisen, such as a high operating temperature and high voltages. For components in the semiconductor industry, suitable insulating materials with excellent dielectric properties are of high importance. In this field, polyimides [2,3] or silicones [4,5] are often used. The applied polymer systems typically show very low water uptake; high water uptake, on the contrary, would influence the dielectric properties drastically and eventually degrade the polymer, which can destroy the device. Due to this reason, the polymers used are hydrophobic with a very limited number of polar functionalities.

Another important factor is the adhesion of a given insulator on metal surfaces. Typically, copper surfaces are very challenging with respect to interaction with the coating and sufficient adhesion. Different techniques have been designed to enhance this interaction: Plasma treatment is one strategy to change the chemical surface of a given material. By plasma processes, different functional groups such as oxygen-containing polar functionalities can be formed on the substrate surface, increasing the polymer-metal interaction. Another possibility is the altering of the polymer system by, e.g., blending it with suitable additives.

For the adhesion enhancement on a copper surface, the introduction of amine groups into the polymer shows great impact, and, hence, azoles like benzimidazole are frequently used. These azoles are capable of forming complexes with different metal atoms such as copper. This interaction, consequently, enhances the adhesion properties of the polymer. However, azoles are polar additives, and, hence, influence the polarity of the whole polymer-based insulator. An increased polarity influences different properties besides adhesion, like water uptake and the dielectric behavior.

Besides, the formed complexes can affect the ion-conducting behavior of a given matrix. If additives such as benzimidazoles are blended into a polymer system, they are not fixed at a given location and can migrate through the polymer matrix. This is also valid for the corresponding complexes and, as a result, the unfavored ion conductivity can be enhanced. To minimize a migration through the polymer system, covalent embedment of the additives can be a potent strategy.

As photolithography plays a great role in the semiconductor industry, polymeric materials, which can react under UV irradiation, are of great interest. Different suitable polymeric systems are on the market, showing either polarity changes or degradation under UV irradiation, which make them soluble, or crosslinking reactions, which makes them insoluble. Due to these reactions, a pattern can be transferred from a mask onto a given polymer film via photolithography. High-intensity light sources are needed for these processes in order to get sufficiently high resolution.

A versatile polymer class, capable of reacting under UV irradiation, is poly(2-oxazoline)s. Via a living cationic ring-opening polymerization, a wide range of different homopolymers or copolymers can be produced with low molecular weight distribution. It is possible to introduce double bonds into the polymer as side-chain functionality by (co-)polymerizing the corresponding 2-oxazoline monomer. This double bond can undergo thiol-ene click-reactions with mono- or multifunctional thiols. This click-reaction is a very potent reaction for the insertion of functionalities into a polymer. With this reaction, polymer chains can be crosslinked if oligofunctional thiols are used, yielding a dense three-dimensional polymer network. With a suitable photoinitiator, this thiol-ene click-reaction can be induced by UV light, combining the advantages of click-chemistry with the advantages of UV-induced reactions.

Besides, also suitable additives can be covalently embedded into a given polymer system utilizing the thiol-ene click-reaction. Due to covalent embedment, the additives are limited in their mobility, decreasing a possible migration. Besides, the additives cannot be washed out of the polymer matrix. Nevertheless, the thiol-ene click-reaction is not limited to poly(2-oxazoline)s. A wide range of polymers can undergo this reaction for a crosslinking, like poly(butadiene) or suitable silicones: If these polymers contain a double bond, UV-induced crosslinking with a suitable multifunctional thiol is possible.

2. Scope and Motivation

For the enhancement of the adhesion of a polymer coating on a metal surface, as it is needed in the semiconductor industry, azole-based additives can be used, due to the formation of complexes. However, it is assumed that the ion migration behavior through the polymer system is influenced (enhanced) by this strategy.

The scope of this work, hence, was to investigate the ion diffusion and ion migration behavior of different polymer systems, which were to be blended with polar additives. Therefore, two different polymer systems were chosen, namely a 2-oxazolin-based copolymer and a polysiloxane. Four different additives, two based on imidazoles and two based on urea, were chosen. These additives are known to be capable of forming complexes with a variety of metal ions like copper.

For the investigation on the ion migration and diffusion, blended polymer films of the two polymer systems, which contained the chosen additives, were prepared as well. Suitable additives were covalently embedded into the polymer matrix by the thiol-ene click-reaction. Consequently, the mobility of the additives in the polymer was expected to be minimized. In order to establish structure-property relationships, the influence of these additives was compared to the influence of non-covalently embedded additives.

For the quantification of ion diffusion and migration, polymer films were to be used as membranes in a permeation cell that was filled with NaCl electrolyte solution. The amount of sodium ions that migrated through the membrane was to be quantified by ICP-OES in order to investigate a possible migration enhancement in the blended polymer films. Besides, impedance measurements were to be performed, using an aqueous NaCl solution to investigate the time-dependent electronic conductivity of the different polymer films.

3. State of the Art

3.1 Conducting Polymers

Classical polymers are commonly known for their insulating behavior, as they are used in different electronic devices as insulators and, of course, also for cable insulations. However, a wide range of different polymeric materials with many different properties is available nowadays. A simple way to alter the properties of a material is by blending it with different substances. For instance, carbon-based fillers are a widely used additive to alter the properties of a given polymer. With the addition of graphite, or carbon nanotubes, the polymer blend can obtain the electrically conducting behavior of the filler [66]. This use of fillers also can affect other properties of the final product, for instance the mechanical properties of the polymer can be altered drastically, especially with high filler content.

Furthermore, polymers which are conductors without the use of additives were discovered: A conjugated system of single and double bonds has to be present like in poly(acetylene), which was the first polymer of its kind. With the use of a strong oxidant or reductant, defects are introduced into the polymer main chain, enabling electrical conductivity [6].

3.1.1 Ion-Conducting Polymers

The main topic of this work was the investigation of the ionic conductivity behavior of polymer systems. Many different polymers show an excellent ion conductivity, which has been utilized in different systems.

In battery systems like lithium ion batteries, a polymer electrolyte can be used. Therefore, a suitable salt is dissolved within the polymer matrix like, e.g., poly(propylene oxide) [7].

A versatile polymer class showing great interaction with lithium ions is poly(ethylene glycol) PEG due to the high abundancy of oxygen atoms; this polymer can be applied as solid electrolyte. As lithium accumulators are of great current interest, a lot of research addresses this topic these days. Different derivatives of poly(ethylene

glycol) meet the necessary requirements. Due to the structure of PEG mimicking crown-ethers, migration of lithium ions between the electrodes is possible [8].

Sulfonated polyimide membranes are used for instance in fuel cells, enabling the protons to move [9]. The structure of the most widely used polymer membrane in fuel cells, NAFION [10-12], is shown in Figure 1. From the sulfonic acid group present, a proton can be easily abstracted, yielding an ionomer [13]. Ionomers are polymers that show distinct ionic character, which affects the mechanical and thermal properties.

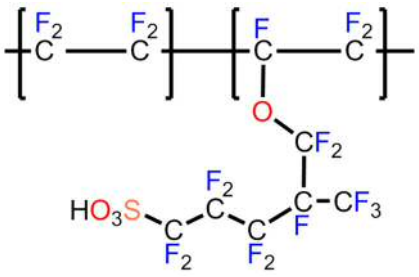

Figure 1: Structure of NAFION.

Via copolymerization, different kinds of ionomers can be produced. Zhang et al. reported the incorporation of ionomer functionality into poly(methyl pentene), using a Ziegler-Natta catalyst (Figure 2). The introduced amino groups act as ionomer, influencing the mechanical as well as the electrical properties of the polymer [14].

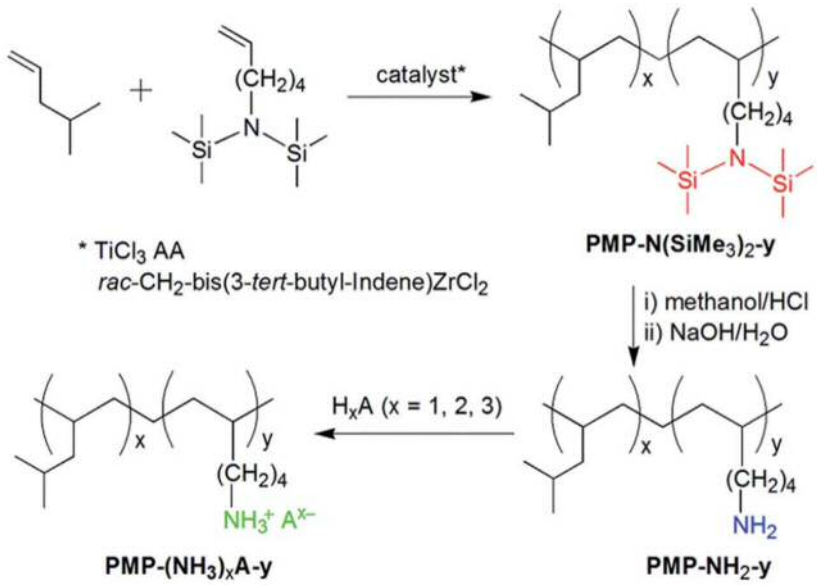

Figure 2: Scheme for the introduction of an ionomer group into a PMP copolymer [14].

Other commercially widely used ionomers are ethylene acrylic acid copolymers, which show excellent adhesion on, e.g., alumina due to the ionic character. They are widely used as inert packaging material [15].

3.1.2 Influences on the Adhesion Properties

The adhesion properties of a polymer system are often challenging in the semiconductor industry. Many polymers, which are applied as insulators, show poor adhesion on copper surfaces and, hence, are often modified by different additives. One well-known additive class to enhance the adhesion on a copper surface is azoles. Azoles contain one nitrogen atom in a five-membered heterocyclic ring and, in addition, at least one other heteroatom; imidazole contains two nitrogen atoms (Figure 3). The azole ring, and especially the imidazole ring, can interact with a given copper surface [16-19]. Wu et al. showed that this interaction is mainly due to the nitrogen atom present in the ring, capable of forming a complex with copper [16].

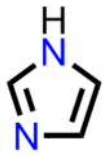

Figure 3: Structure of imidazole.

Benzimidazole can form a polymer-like layer on copper surfaces with thicknesses of 100 Å. This imidazole film can act as coupling agent between copper and an epoxy polymer matrix [20, 21]. Lee et al. showed that the peel strength of polyimides on a copper surface can be more than doubled due to the formation of complexes between the copper surface and the (eventually) azole-containing polyimide [22]. The copper-azole complex cannot only be used as adhesion promoter, but also for corrosion inhibition [23].

As already mentioned hereinabove, the introduction of an additive into a polymer matrix usually affects many different properties. Different azoles are used in polymer inclusion membranes for the selective extraction of, e.g., copper ions from solutions containing different metal ions [24]. Ulewicz et al. concluded that after the formation of copper-azole complexes, they can diffuse through a suitable membrane and,

therefore, selective copper extraction is enabled [25]. Mitiche and colleagues showed that suitable azoles in a polymer matrix can act as copper extractant. They performed transport experiments in permeation cells showing the capability of azole carriers for the extraction of copper [26].

In the semiconductor industry, hence, unwanted copper ion diffusion through the polymeric coating has to be considered if azole-containing polymers are used as insulators. Potentially, even dendrite formation can occur, which severely affects the dielectric properties of an insulating film.

Other additives that are capable of forming complexes with copper are assumed to have an impact on the adhesion properties of a polymer on a copper surface as well. Derivatives of urea are known to be able of forming such complexes [27-29] as they, similar to azoles, contain nitrogen atoms. Besides, also the oxygen atom is directly involved in the formation of complexes.

3.2 Photolithography

One of the most fundamental techniques in the semiconductor industry is photolithography for the production of integrated circuits. Photolithography is a powerful tool to form precise patterns on substrates. During the photolithographic process, a substrate that is coated with a photoresist gets illuminated through a mask and, consequently, the pattern of the mask is reproduced. The relevant steps for the photolithographic process are presented in Figure 4 [30].

From the chemical point of view, the most interesting step is the curing of the photoresist. For this step, a high-intensity light source, like a UV lamp, is needed. Mercury lamps have dominated this field for many years, as they show several strong peaks in the emission spectra between 300 and 450 nm. Commonly used are the emissions at 436 nm (so-called g-line) [31] and 365 nm (so-called i-line) [32], which are selected by suitable filters.

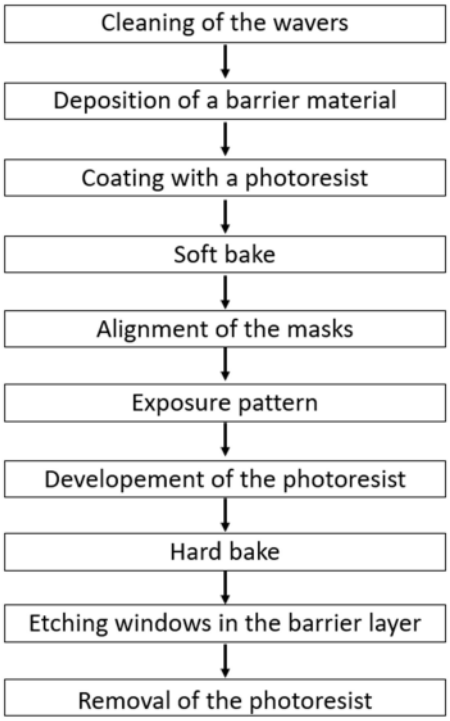

Figure 4: Typical process steps in photolithography [30].

However, the resolution and accuracy of the produced patterns is limited by the wavelength of the light source. The feature size F is described by Equation 1 [33],

$$F = k_1 \cdot \frac{\lambda}{n \cdot \sin\theta} \qquad (1)$$

in which λ represents the used wavelength, sinθ represents the numeric aperture of the system, and k_1 is a parameter of the photoresist. The lower the wavelength, the lower the feature size F, and, hence: The resolution increases with decreasing wavelength. The parameter k usually has a value approx. 0.4 for a modern photoresist, although the theoretical minimum would be around 0.2-0.3 [34]. The numeric aperture of the system is mostly dependent on the quality of the used lens system.

Another important factor is the depth-of-field DOF, which is described by Equation 2,

$$DOF = k_2 \cdot \frac{\lambda}{(n \cdot \sin\theta)^2} \qquad (2)$$

in which k_2 represents the Rayleigh-coefficient, which is determined by the process itself. Again, the numeric aperture is part of this equation. This means that the depth-

of-field as well as the feature size are strongly dependent on the used lens system; however, the used light affects these parameters most significantly.

Concomitantly, the trend leads towards light sources operated at smaller wavelengths and, thus, higher energies. Excimer lasers [35,36] meet these requirements, as wavelengths of 126 nm can be reached [37]. In excimer lasers, a noble gas reacts with a halogen, producing an excited dimer (excimer; e.g. KrF^*), which has a life span of roughly 20 ns until it relaxes to the ground state, emitting photons of a specific wavelength (249 nm for KrF^*) [38].

In principle, two different photo resists are available for photolithography – positive and negative resists (Figure 5). Negative resists become insoluble during the illumination step, reproducing a negative image of the used mask, while a positive resist becomes (more easily) soluble after illumination, reproducing a positive image of the mask. The etching is usually performed by applying wet chemical methods [39, 40] or plasma technologies [41].

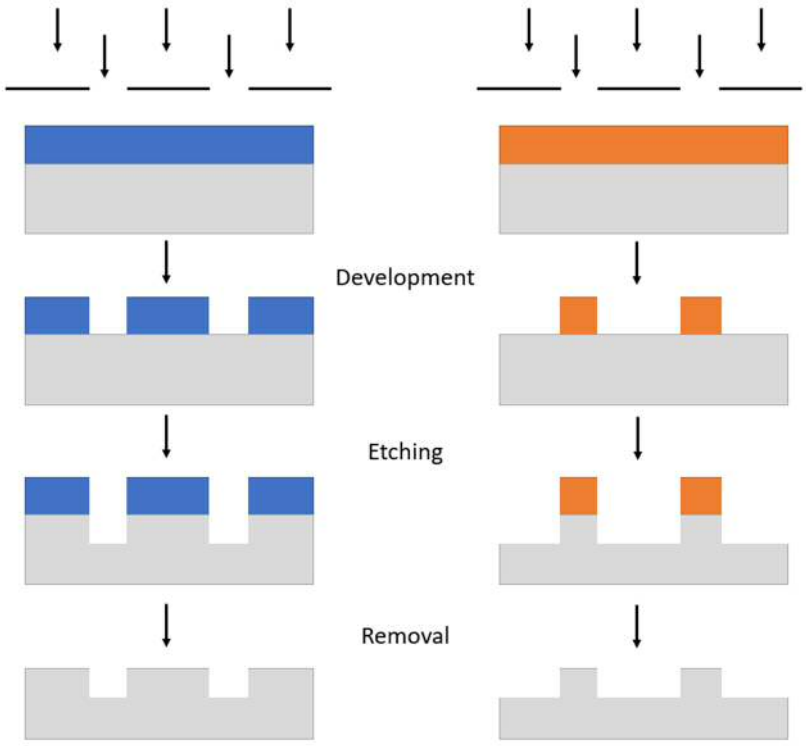

Figure 5: Comparison of a positive and a negative photoresist.

3.3 2-Oxazolines

2-Oxazolines consist of a 5-membered heterocyclic ring with one nitrogen and one oxygen atom at positions 1 and 3, and a double between the nitrogen and the C^2 carbon atom. Different synthetic routes are known for the synthesis of 2-oxazolines.

3.3.1 Synthetic Pathway: The Henkel patent

A very potent strategy for the synthesis of 2-oxazolines is described by the Henkel patent [42]. Published in 1990, this patent describes the synthesis of 2-oxazolines from fatty acids and 2-aminoethanol in the presence of a titanium catalyst [e.g. $Ti(OBu)_4$]. The reaction scheme is shown in Figure 6. This synthetic procedure is especially suitable for fatty acids with 7-21 carbon atoms. Great advantages of this synthesis are the facts that no solvent is needed for this reaction and that the fatty acids are mostly produced from different seed oils, making this reaction renewable.

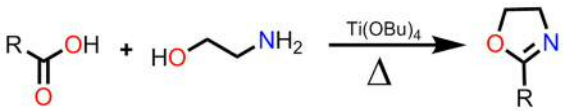

Figure 6: Reaction scheme for the synthesis of 2-oxazolines according to the Henkel Patent [42].

3.3.2 Synthetic Pathway: Synthesis according to Witte and Seeliger

A different reaction pathway was presented by Witte and Seeliger [43]. Especially 2-oxazolines with cyclic or aromatic substituents can be synthesized. A cadmium catalyst is needed for this reaction (Figure 7). Witte and Seeliger presented a broad range of possible side-groups R^1, while R^2 is either a hydrogen atom or a methyl group. For many monomers, a solvent-free synthesis is possible. For purification, the product has to be distilled by vacuum distillation.

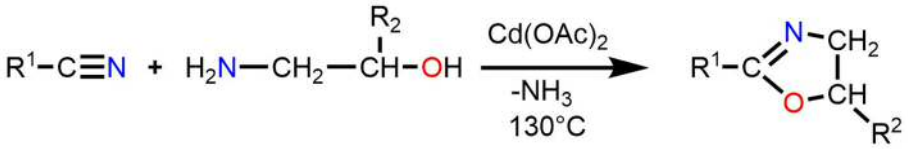

Figure 7: Synthesis of 2-oxazolines according to Witte and Seeliger [43].

3.3.3 Polymerization of 2-oxazolines

2-Oxazolines can be polymerized via the cationic ring-opening polymerization CROP in the presence of a suitable cationic catalyst, which was first described in 1966 (Figure 8) [44,45].

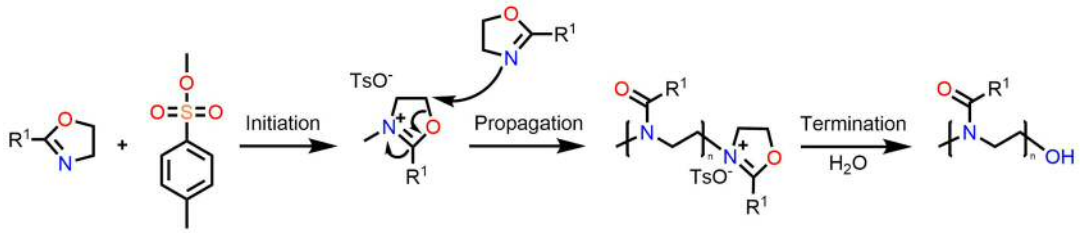

Figure 8: Reaction scheme for the living cationic ring-opening polymerization of 2-oxazolines [50].

For many syntheses, the polymarization rate can be a bottleneck, resulting in very long reaction times [46]. In the case of 2-oxazolines, this phenomenon has limited their industrial importance in the early days. Notably, it is possible to polymerize 2-oxazolines in microwave reactors, and, using microwave-assisted synthesis, the reaction times can be reduced from hours to minutes in many cases, besides reducing possible side-reactions and increasing yields [47-49]. This reduction of the reaction time is due to the high possible reaction temperature under autoclave conditions, as the boiling point of the liquid is no limiting factor anymore. Wiesbrock et al. investigated the CROP reaction of 2-oxazolines, using a microwave reactor and observed an acceleration factor of up to 400 for the polymerizations [50].

The polymerization of 2-oxazolines was proven to have a pseudo-living character, meaning that this polymerization technique is very controlled. Side-reactions are minimized and chain-transfer reactions are drastically reduced under living conditions, resulting in very narrow molecular weight distributions. GPC studies showed a linear correlation of the number-average molecular weights and the monomer conversion, illustrating the livingness of the polymerization [51].

Due to the living character, block copolymers can be synthesized with defined chain length. Molecular weight distributions for different 2-oxazoline-based triblock-polymers have been investigated, showing dispersity indices of approx. 1.2 [52].

3.4 Thiol-Ene Click-Reactions

Polymeranalogous reactions are a powerful tool to modify the properties of a given polymer chain. Functional groups can be added or altered, changing the overall properties of the polymer. An example of industrial importance is the production of poly(vinyl alcohol). For a 'classical' polymerization, vinyl alcohol would need to be chosen as monomer, which, however, is non-existent under standard conditions as the tautomeric equilibrium lies on the side of the acetaldehyde. Therefore, in a first step, poly(vinyl acetate) is produced from vinyl acetate by radical polymerization. In a subsequent step, poly(vinyl acetate) is saponified or trans-esterified, yielding the targeted poly(vinyl alcohol) (Figure 9) [53].

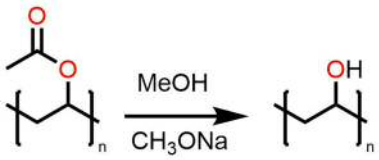

Figure 9: Polymeranalogous reaction of poly(vinyl acetate) yielding poly(vinyl alcohol).

A plethora of polymeranalogous reactions is known. One very interesting example thereof is the thiol-ene click-reaction (Figure 10). Click-reactions typically show very little side-products and selective and quantitative conversion. In 2001, Sharpless et al. presented a widely accepted concept for this new class of reactions [54]: The insensitivity against oxygen, the mild reaction conditions and the possibility of water as solvent are among the advantages of click-chemistry.

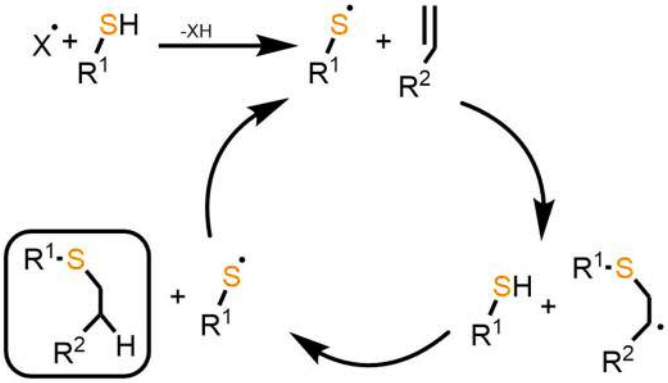

Figure 10: Reaction mechanism of the thiol-ene click-reaction.

In the course of the thiol-ene click-reaction, a carbon-carbon double bond and thiol functionality have to be present. Thiol-ene click-reactions are initiated radically. Very often, this reaction is UV-induced, which shows many advantages such as local as well as temporal resolution [55]. Nonetheless, also thermally initiated thiol-ene click-reactions find their applications [56]. The initiator radical can abstract a proton from a thiol group, yielding a thiyl radical, which can attack a C=C double bond. Thereby, a sulphur-carbon bond is formed, and the radical at the neighboring carbon atom can abstract a proton from a nearby thiol group, reproducing the thiyl radical.

3.4.1 Introduction of different functionalities

With thiol-ene click-reactions, polymer properties such as the solubility or the polarity can be changed. In polymer systems like poly(butadiene) or poly(allyl methacrylate)s, double bonds are present in the side-chains, which can react with a suitable thiol. For instance, a long-chain alkanethiol can be introduced to change the polarity [57]. Also hydroxy groups or even carboxy groups for further reactions can be introduced [58].

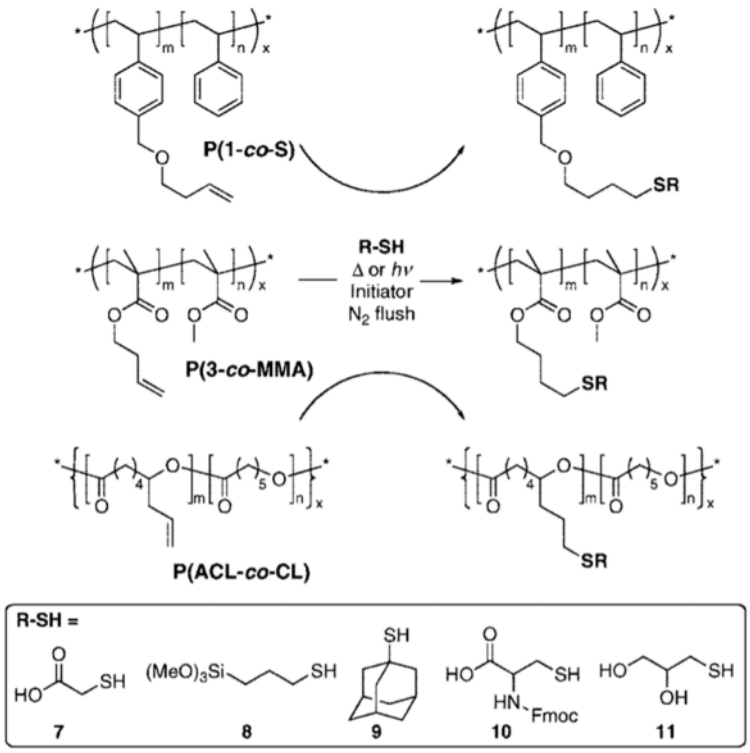

Figure 11: Possibilities for the functionalization of polymers by the thiol-ene click-reaction [58].

2-Oxazolines also obtain double bonds if they are produced from a corresponding fatty acid such as undec-10-enoic acid. Consequently, 2-oxazoline-base homo- or copolymers containing double bonds in their side-chains can be produced. Poly(decenyl-2-oxazoline) can be modified by thiol-ene click-reactions with thiols such as *n*-dodecanethiol or crosslinked if dithiols of multifunctional thiols are used [59].

3.4.2 Crosslinking via the Thiol-Ene Click-Reaction

Crosslinking is of special interest, as the polymer system gets insoluble in any organic solvent due to the crosslinking. Depending on the amount of double bond functionalities in a given polymer chain and the amount of thiol functionalities of the crosslinker, the density of the crosslinked polymer system can be adapted. As the thiol-ene click-reaction can be UV-induced, negative photoresists with resolutions of 2 µm can be produced from poly(2-oxazoline)s [60].

3.5 Zeta Potential Measurements

The charges at interfaces can be described by the zeta potential. Solid-liquid interfaces are often analyzed using zeta potential measurements. With the electric double layer EDL concept, the zeta potential can be described (Figure 12).

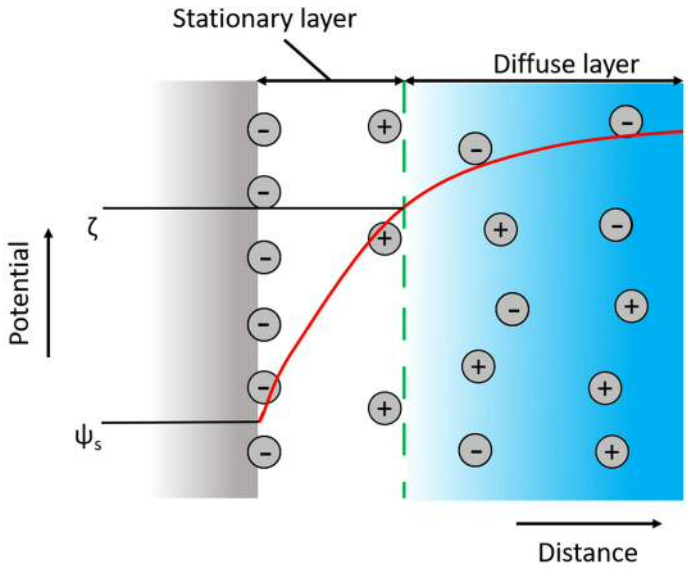

Figure 12: Scheme of the electric double layer EDL concept.

Surfaces contain charges when they are in contact with aqueous solutions and, hence, the charge distribution is different than the charge distribution in the liquid phase. Due to this difference, a charge potential is formed, which depends on the distance to the solid surface. Two layers are described by the EDL, namely the stationary and the diffuse layer, which compensate the surface charges. The zeta potential ζ is the potential at the border of the stationary and the diffuse layer. This boundary is the so-called shear plane, indicating that the diffuse liquid layer moves relative to the stationary liquid phase. The zeta potential is dependent on the distance of the shear plane to the solid surface and the properties of the present liquid phase. For the formation of a surface charge between a liquid solution and a solid two mechanisms are of great significance: acid base reactions and the adsorption of neutrally charged water ions.

Carboxylic acid functionalities on a surface can protonate surrounding water molecules; on the other hand, alkaline functionalities like amino groups can get protonated by water molecules. The surface charges of a solid in contact with an aqueous solution are therefore dependent on the surface functionality of the solid. Certainly, the pH-value plays an important role in this context, as it mainly directs possible acid-base reactions.

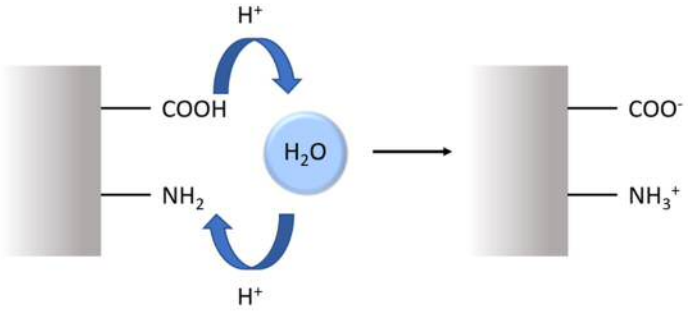

Figure 13: Acid-base reactions at a solid surface in contact with an aqueous liquid.

Zeta potential techniques are often discussed in the context of nanoparticles, as their surface is of great interest in many fields nowadays. Nanocomposites have already found applications in many fields, and a lot of research is performed in this area, especially the functionalization of nanoparticles is interesting and, therefore, zeta potential measurements are a powerful characterization tool.

However, also other surfaces can be characterized with the zeta potential using the streaming potential technique. For this technique, a channel filled with an aqueous solution is needed. As already described, surface charges form on a solid when it is in contact with a liquid, which are compensated by countercharges in the solution, resulting in an equilibrium state. When the liquid in the channel starts to flow, the countercharges are sheared relative to the surface charges in the direction of the flow. Charges are moving through the channel, resulting in a measurable so-called streaming potential, which can be detected. The size of the channel as well as the applied flow rate of the liquid phase has a great impact on this potential [61].

3.6 Contact Angle Measurements

The contact angle can quantify the polarity of a surface: A liquid drop is placed onto a solid surface, and the contact angle is measured at the three-phase boundary (solid, liquid, gas) (Figure 14). Assuming that the liquid is water, a hydrophilic surface is shown (the contact angle is low). Contact angles below 90° indicate good wetting, while contact angles above 90° represent non-wetting behavior.

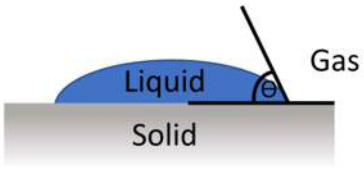

Figure 14: Visualization of the principle of contact angle measurements.

The contact angle is strongly dependent on the polarity of the liquid. Usually, water and diiodomethane are used, but also ethylene glycol can be applied. From the contact angles of a substrate with different liquids, the surface energy can be calculated. The wettability of a substrate is also dependent on the morphology of the surface. A nanostructure can have great impact on the contact angles of different liquids, like it is known for the lotus effect. For polymeric systems such morphologies are already described in literature, like for 2-oxazolines containing nonyl side groups. AFM measurements revealed an increased surface roughness, which has also been correlated to a change in the surface energy [62].

4. Results and Discussion

4.1 Monomer Synthesis: 2-Dec-9'-enyl-2-oxazoline (Dec$^{=}$Ox)

The synthesis of the 2-dec-9'-enyl-2-oxazoline monomer was performed according to the Henkel patent [42] from undec-10-enoic acid and ethanolamine with the use of titanium(IV) butoxide as a catalyst (Figure 15).

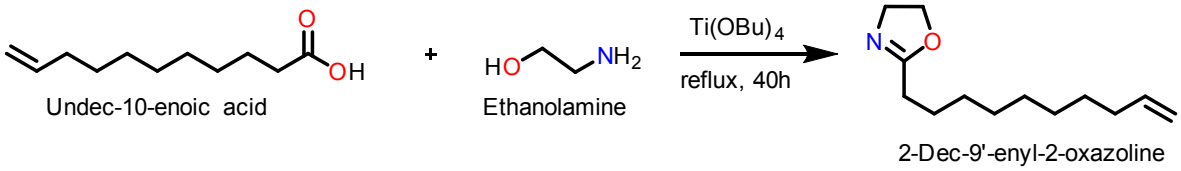

Figure 15: Reaction scheme for the synthesis of 2-dec-9'-enyl-2-oxazoline.

The crude product mixture was purified by vacuum distillation (180 °C, <4 mbar) and column chromatography on silica to remove side-products. The purity was determined by ^{1}H-NMR spectroscopy (Figure 16). No by-products could be detected; the shifts and integrals of the peaks are in best alignment with the given structure.

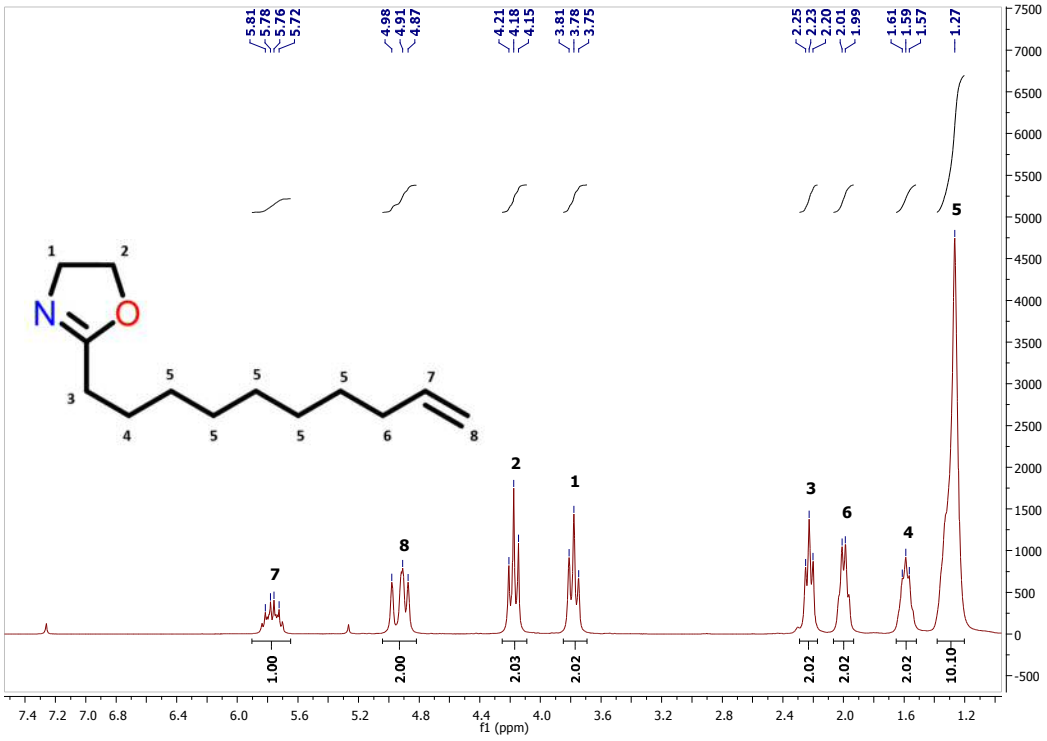

Figure 16: ^{1}H-NMR spectrum of 2-dec-9'-enyl-2-oxazoline.

4.2 Monomer Synthesis: 2-Nonyl-2-oxazoline (NonOx)

The synthesis was performed according to the Henkel patent [42] with decanoic acid and ethanolamine as reactants and titanium(IV) butoxide as catalyst (Figure 17).

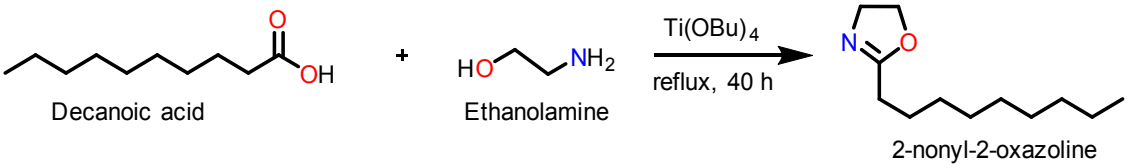

Figure 17: Reaction scheme for the synthesis of 2-nonyl-2-oxazoline.

The crude product mixture was purified by vacuum distillation (180 °C, <4 mbar) and column chromatography on silica to remove side-products. The purity of the product was determined by ^{1}H-NMR spectroscopy (Figure 18). No by-products could be detected; the shifts and integrals of the peaks are in best alignment with the given structure.

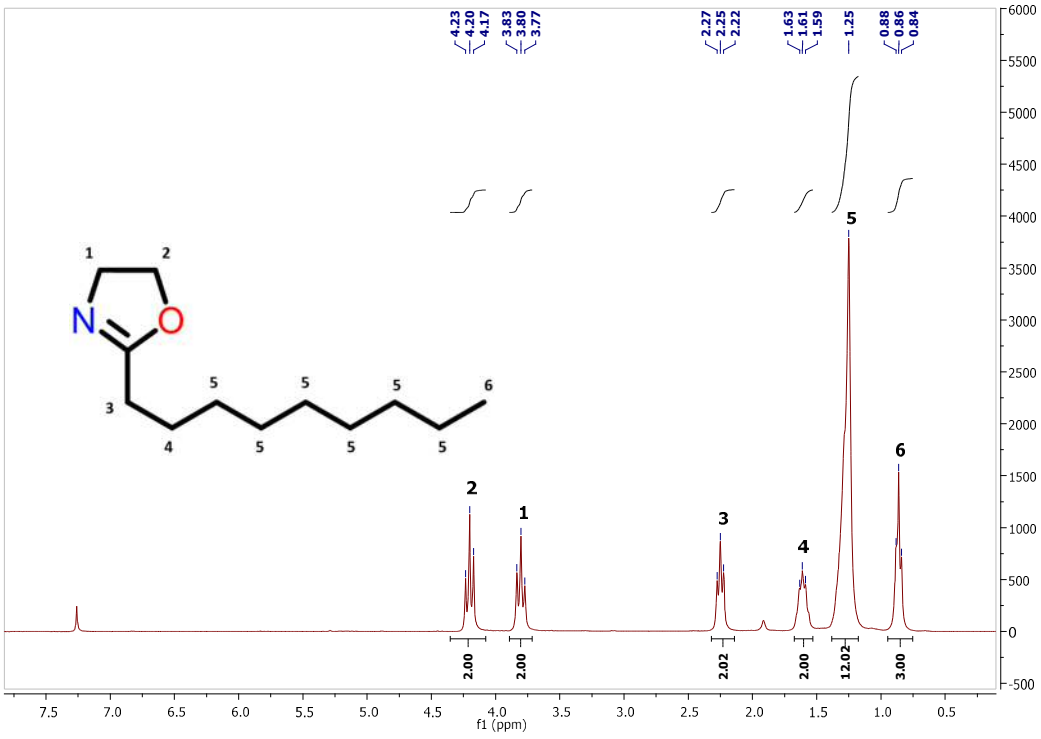

Figure 18: ^{1}H-NMR spectrum of 2-nonyl-2-oxazoline.

4.3 Microwave-Assisted Synthesis of Poly(2-nonyl-2-oxazoline)-*stat*-poly(2-dec-9'-enyl-2-oxazoline)

For the synthesis of the abovementioned copolymer (Figure 19), the pseudo-living cationic ring-opening polymerization was employed. The polymerization was performed in a microwave reactor; as the reaction temperature was not limited by the boiling point of the solvent, it was possible to operate at high temperatures, reducing the reaction time notably. It is important to mention that the polymerization is pseudo-living, meaning that the initiation step is faster than the propagation step, resulting in a narrow molecular weight distribution.

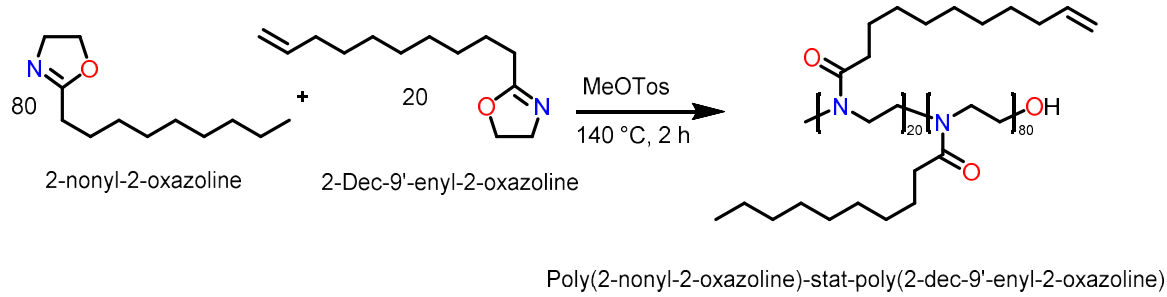

Figure 19: Scheme for the synthesis of poly(2-nonyl-2-oxazoline)-stat-poly(2-dec-9'-enyl-2-oxazoline).

For the polymerization, 2-nonyl-2-oxazoline and 2-dec-9'-enyl-2-oxazoline were weighed into a microwave vial in a molar ratio of 4:1 and dissolved in acetonitrile. In order to obtain a polymer product with a chain length of 100 repetition units, the ratio of methyl tosylate to monomer was set to 1:100. The reaction was performed at 140 °C for 2 h under autoclave conditions yielding a colorless solid product. The remaining solvent has been removed by rotary evaporation.

The purity of the product and ratio of 2-nonyl-2-oxazolin to 2-dec-9'enyl-2-oxazoline was determined by ^{1}H-NMR spectroscopy (Figure 20). The peak labeled 4 represents the polymer backbone, consisting of two methylene groups per repetition unit. As polymer chains with 100 repetition units were targeted, the integral was set to 400. The peaks labeled 1 and 2 represent the protons of the double bond of the decenyl side-group. The peak labeled 3 represents the protons of the methyl group of the nonyl side group. As the CH_3 group and the two signals for the double bond both account for 3 H-atoms, the ratio of the two different side groups is, as targeted,

62:249 = 1:4. These NMR-results are indicative of the successful synthesis of the copolymer with the targeted ratio of decenyl to nonyl side-groups.

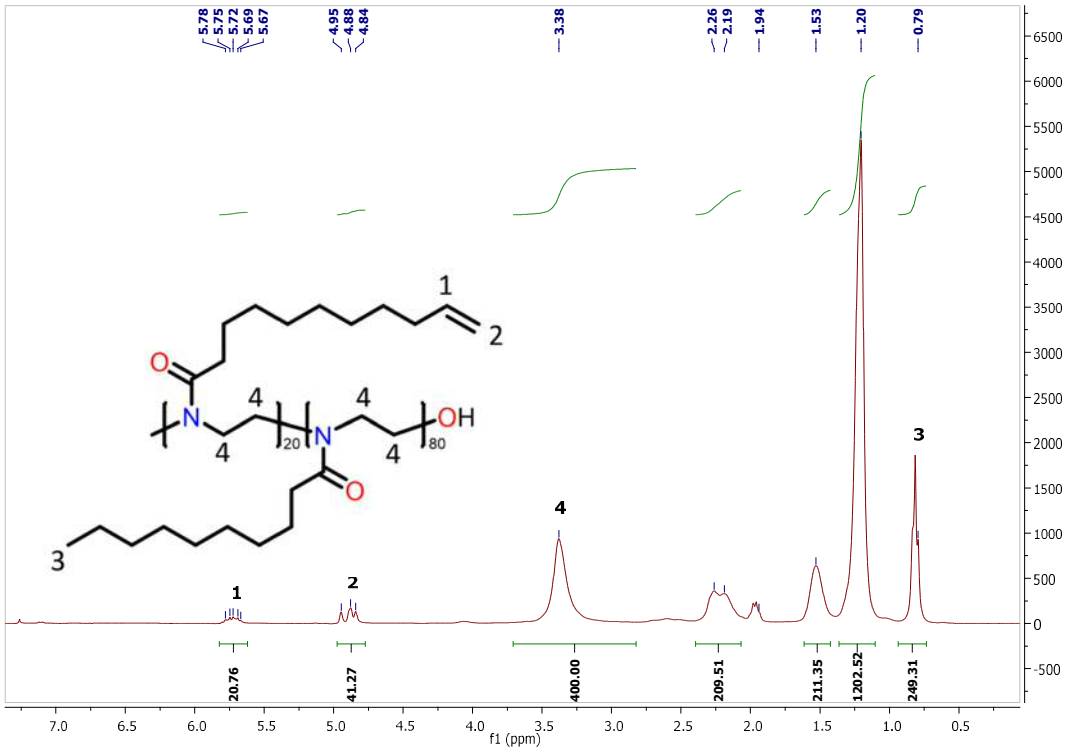

Figure 20: ^{1}H-NMR spectrum of poly(2-nonyl-2-oxazoline-*stat*-poly(2-dec-9'-enyl-2-oxazoline).

4.4 Preparation of the Polymer Films

4.4.1 Crosslinked Polysiloxane Films

For the crosslinking of the polymeric system, the UV induced thiol-ene click reaction was utilized. 1,3-Divinyltetramethyldisiloxane, which contains two double bonds, was cured with a mixture of 2,2'-(ethylenedioxy) diethanethiol and trimethylolpropane tris(3-mercaptopropionate), which contain two and three thiol functionalities, in a mass ratio of 1:4. The crosslinking reaction was initiated by the use of the photoinitiator Lucirin TPO-L (2,4,6-trimethylbenzoylphenyl-phosphinic acid ethyl ester). The highly crosslinked polymeric network is shown schematically in Figure 21.

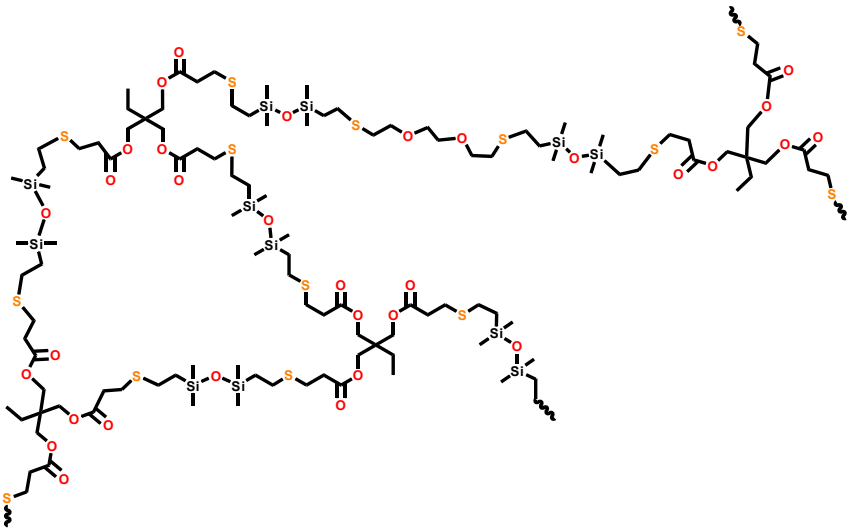

Figure 21: Scheme of the crosslinked network of the produced polysiloxane films.

The reactants were dissolved in 1-methoxy-2-propanol and sonicated for 15 min. The homogenous liquid reaction mixture was then cast onto a flat PET support, distributed to form a thin film, and irradiated with UV light (254 nm, 6 $W \cdot cm^{-2}$) for 30 s. A solid homogenous polymer film formed, which was lifted off the PET support and further illuminated for 5 min. After removing the residual solvent at 80 °C, the film was obtained as colorless solid with a thickness of 150 µm (Figure 22).

Figure 22: Photography of the polysiloxane film (original size: d = 8 cm).

4.4.2 Crosslinked Poly(2-oxazoline) Films

For the crosslinking of the polymeric system, again the UV induced thiol-ene click reaction was utilized. Poly(2-nonyl-2-oxazoline)-*stat*-poly(2-dec-9'-enyl-2-oxazoline) and 2,2′-(ethylenedioxy) diethanethiol were dissolved in a 1:1 mixture of toluene and 1-methoxy-2-propanol, together with the photoinitiator Lucirin TPO-L. The double

bonds of the 2-oxazoline copolymer reacted with the thiol functionalities under UV irradiation (254 nm, 6 $W \cdot cm^{-2}$), yielding a crosslinked polymer network (Figure 23).

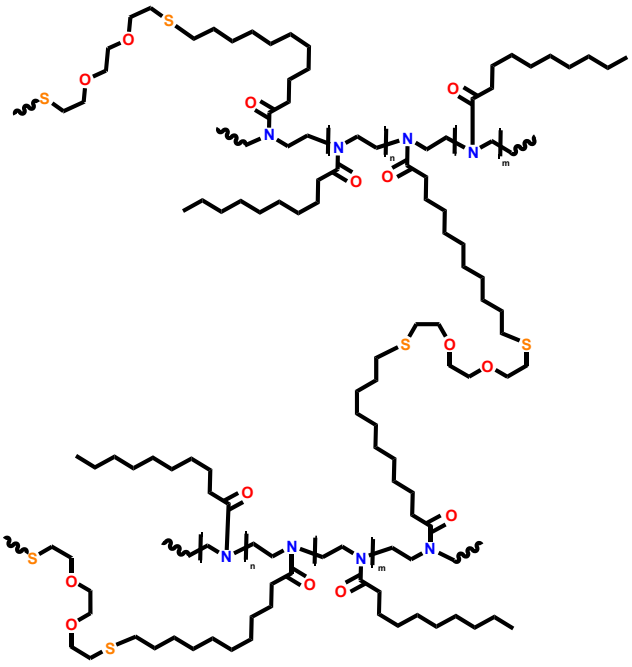

Figure 23: Scheme of the crosslinked network of the poly(2-oxazoline) films.

The liquid reaction mixture was applied onto a PET support and distributed to form a homogenous thin film. During the first seconds of irradiation, a homogenous solid polymer network formed. After 30 s of irradiation, the polymer was lifted off the support and irradiated for another 5 min. After removing the residual solvent at 80 °C, the yellowish film was obtained with a thickness of roughly 150 µm (Figure 24).

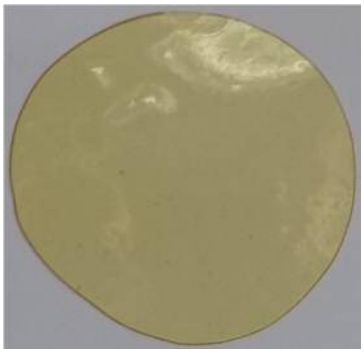

Figure 24: Photography of the poly(2-oxazoline) film (original size: d = 8 cm).

4.4.3 Preparation of the Blended Polymers

Two different types of additives have been used for the preparation of polymer blends. The first class of additives is based on imidazoles (Figure 25). Imidazoles are known to form metal complexes, for instance with copper ions. This phenomenon is already utilized by adding imidazoles to polymeric materials in order to increase the adhesion on copper surfaces. In this work, it was decided to use benzimidazole to investigate its influence on ion migration. However, as it was the aim to also covalently incorporate additives, 2-mercaptobenzimidazole was the substance of choice. The thiol functionality of the 2-mercaptobenzimidazole is capable of reacting with a double bond. Therefore, the covalent attachment can be performed during the curing step of the polymer network via the thiol-ene click reaction. These additives were incorporated into the polymer films with an amount of 5 wt.-%. For 2-mercaptobenzimidazole, the corresponding amount of the thiol crosslinkers 2,2′-(ethylenedioxy) diethanethiol and trimethylolpropane tris(3-mercaptopropionate) had to be adapted in order to apply stoichiometric amounts.

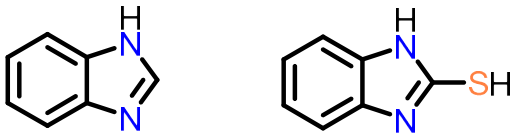

Figure 25: Chemical structures of benzimidazole (left) and 2-mercaptobenzimidazole (right).

The second additive class used is based on urea, as it also forms metal complexes (Figure 26). In this work, *N*-allylurea is used for covalent attachment via the double bond into the polymeric matrix, *N*-methylurea for blending into the network. These additives were incorporated into the two different polymer films with an amount of 5 wt.-% each. For *N*-allylurea, the corresponding amount of the thiol crosslinkers 2,2′-(ethylenedioxy) diethanethiol and trimethylolpropane tris(3-mercaptopropionate) had to be adapted in order to apply stoichiometric amounts.

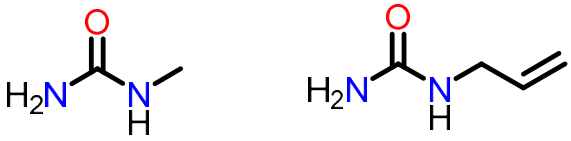

Figure 26: Chemical structures of *N*-methylurea (left) and *N*-allylurea (right).

The preparation of the blended polymer films was performed according to the strategies described in sections 4.4.1 and 4.4.2. With the exception of the polysiloxane film with 2-mercaptobenzimidazole, all blends have been obtained as homogenous films. A possible reason for the precipitation observable in the polysiloxane film with 2-mercaptobenzimidazole might be due to the tautomeric behavior of 2-mercaptobenzimidazole (Figure 27). During the drying of the siloxane film, 2-mercaptobenzimidazol precipitated, indicating that the covalent attachment was not quantitatively successful.

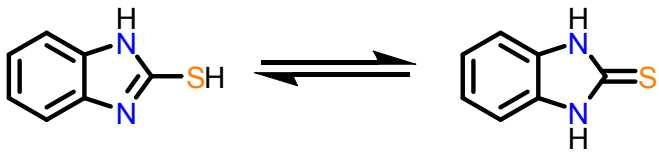

Figure 27: Tautomerism of 2-mercaptobenzimidazol.

In Figure 28 some of the blended polymer films are shown. It is worth mentioning that the polysiloxane blend with *N*-allylurea had a different haptic appearance, softer and more elastic, compared to the other polysiloxane films. The poly(2-oxazoline) films are slightly yellowish.

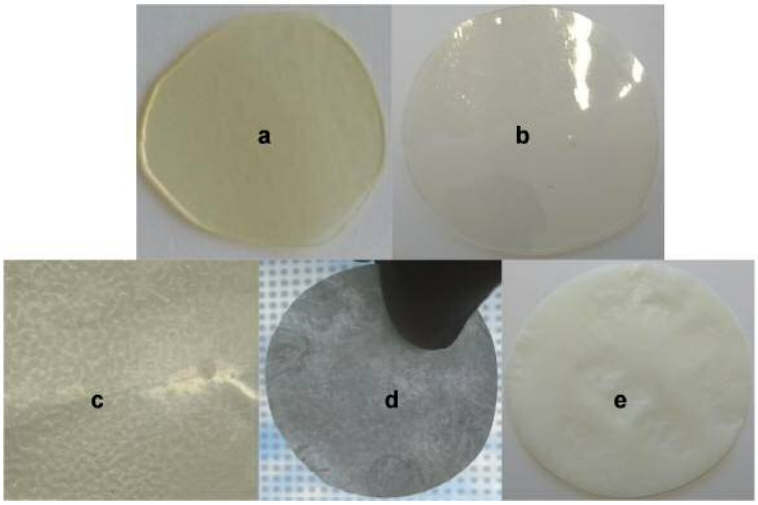

Figure 28: Photographies of the blended polymer films: a) Poly(2-oxazoline) + benzimidazole; b) poly(2-oxazoline) + *N*-methylurea; c) polysiloxane + 2-mercaptobenzimidazole; d) polysiloxane + 2-mercaptobenzimidazole; e) polysiloxane + benzimidazole. Original sizes: d = 8 cm.

4.5 IR Analysis

The polymer films were analyzed by IR spectrometry. The unfilled polymer films were measured in comparison to the blended ones in order to investigate the covalent embedment. The results are also compared to the non-attached additives. The results for the blending of polysiloxane with *N*-allylurea are shown in Figure 29.

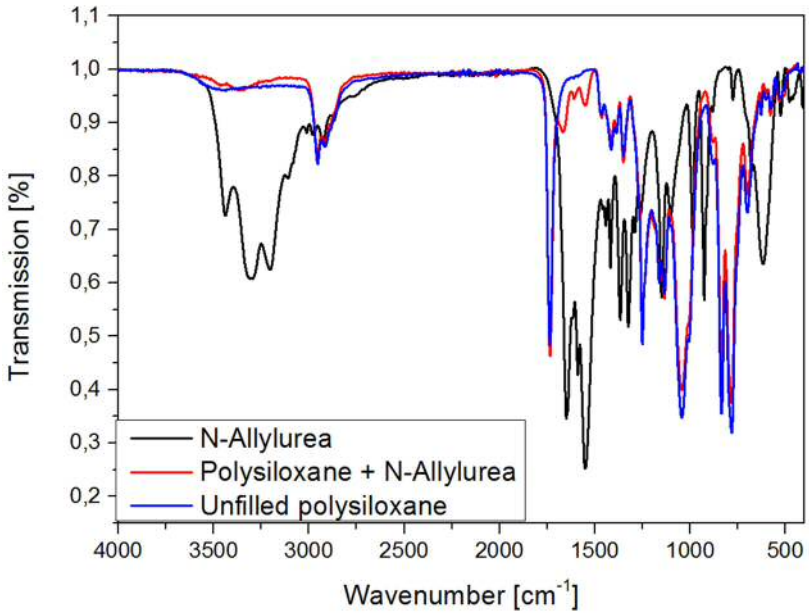

Figure 29: IR spectra of *N*-allylurea in comparison to the corresponding polysiloxane blend and the unfilled polysiloxane.

The black line (Figure 29) represents the additive. Especially the intense peaks in the region of 1500-1650 cm^{-1} can be recognized in the blended polysiloxane, but are absent in the unfilled polysiloxane. The peak at 990 and 925 cm^{-1} represents the double bond of *N*-allylurea. The peak at 990 cm^{-1} overlaps with signals representing the polymer matrix; the other peak, however, is absent in the blended polysiloxane, and covalent embedment of the additive into the polysiloxane matrix by the thiol-ene click reaction can be argued. Apart from these signals, the two spectra of the blended and the pure polysiloxane fit well to each other, indicating that the blending with *N*-allylurea does not disturb the crosslinking of the polysiloxane network.

In Figure 30, the comparison of the IR spectra of the poly(2-oxazoline) system is shown. The IR spectrum of the pure poly(2-oxazoline) network overlaps to great extent with the spectrum of *N*-allylurea. However, the peak at 990 cm^{-1} of the double bond of *N*-allylurea is missing in the spectra of the blended poly(2-oxazoline),

indicating that the covalent embedment of the additive into the polymer matrix was successful. The peak region 3000-3500 cm^{-1}, which represents the amine functionality of *N*-allylurea, can also be identified in the blended system.

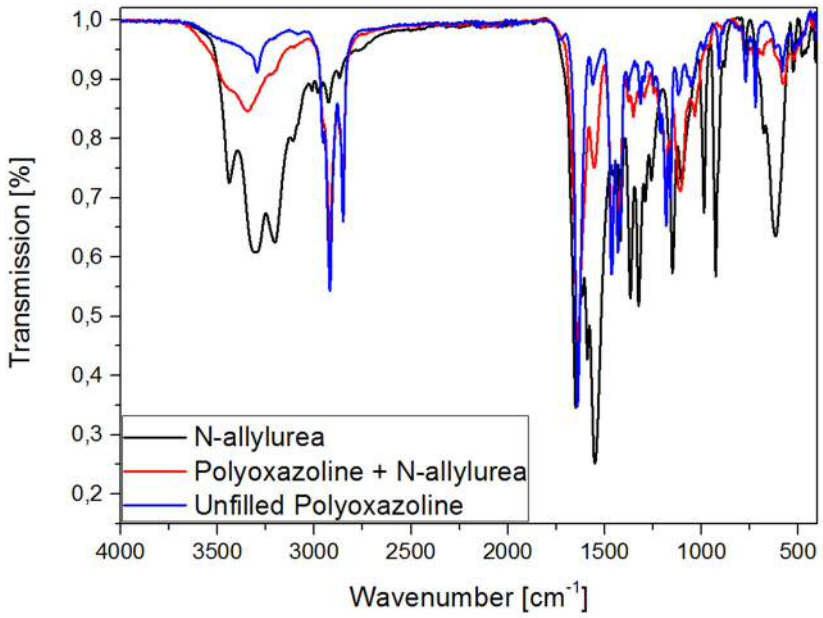

Figure 30: IR spectra of *N*-allylurea in comparison to the corresponding poly(2-oxazoline) blend and the unfilled poly(2-oxazoline).

The covalent embedment of 2-mercaptobenzimidazole as well was investigated with IR spectroscopy. Again, the unfilled polymer films were measured in comparison with the blended ones and 2-mercaptobenzimidazole (these spectra were fitted with a spline function). The comparison of the IR spectra for the polysiloxane, blended with 2-mercaptobenzimidazole is shown in Figure 31. The thiol functionality is represented by a peak in the region of 2500-2600 cm^{-1}. The spectrum of the unfilled polysiloxane does not show any peaks in this region; however, for the blended polymer, the peak is still present. This indicates that 2-mercaptobenzimidazole is not quantitatively incorporated covalently into the polysiloxane matrix, coinciding with the observation that 2-meraptobenzimidazole precipitated during the preparation of the blended polysiloxane films.

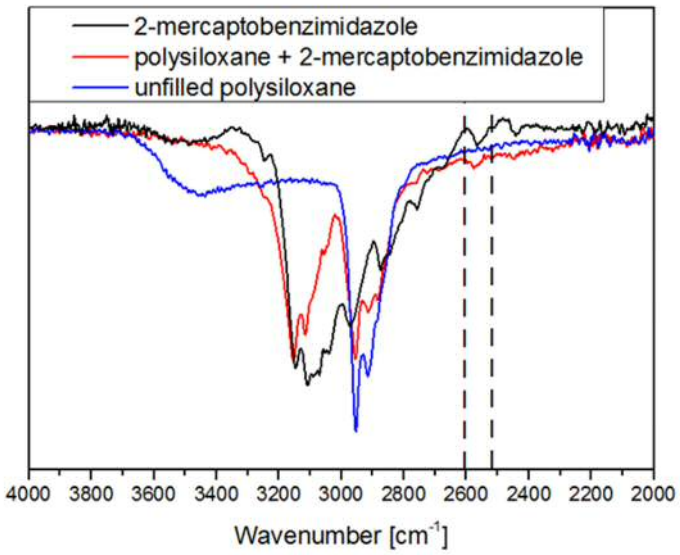

Figure 31: IR spectra of 2-mercaptobenzimidazole in comparison to the corresponding polysiloxane blend and the unfilled polysiloxane.

2-Mercaptobenzimidazole was also blended into the poly(2-oxazoline) films (these spectra were fitted with a spline function) (Figure 32). The typical thiol-peak for the 2-mercaptobenzimidazole in the region of 2500-2600 cm^{-1} is not present in the blended poly(2-oxazoline) matrix and the unfilled poly(2-oxazoline), indicating that the covalent embedment was successful. In comparison to the polysiloxane blend, no precipitation of the additive has been observed during the film preparation.

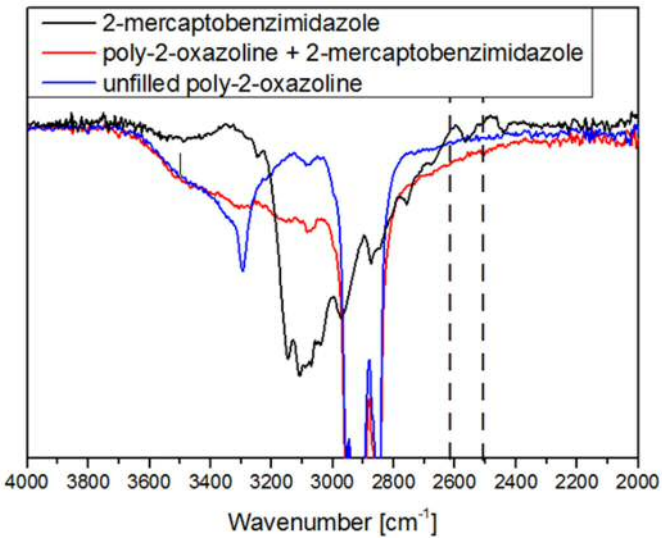

Figure 32: IR spectra of 2-mercaptobenzimidazole in comparison to the corresponding poly(2-oxazoline) blend and the unfilled poly(2-oxazoline).

4.6 SEM-EDX Analysis

The prepared polymer films have also been investigated by SEM-EDX measurements. By using secondary electron microscopy, the morphology of a given substrate and inhomogeneities can be investigated. Energy-dispersive X-ray spectroscopy determines the chemical composition of a substrate. Prior to the analysis, the polymer film samples were coated with a thin gold layer to make the measurements possible. In Figure 33 and 34, SEM images of the poly(2-oxazoline) films with different incorporated additives are shown and compared to each other.

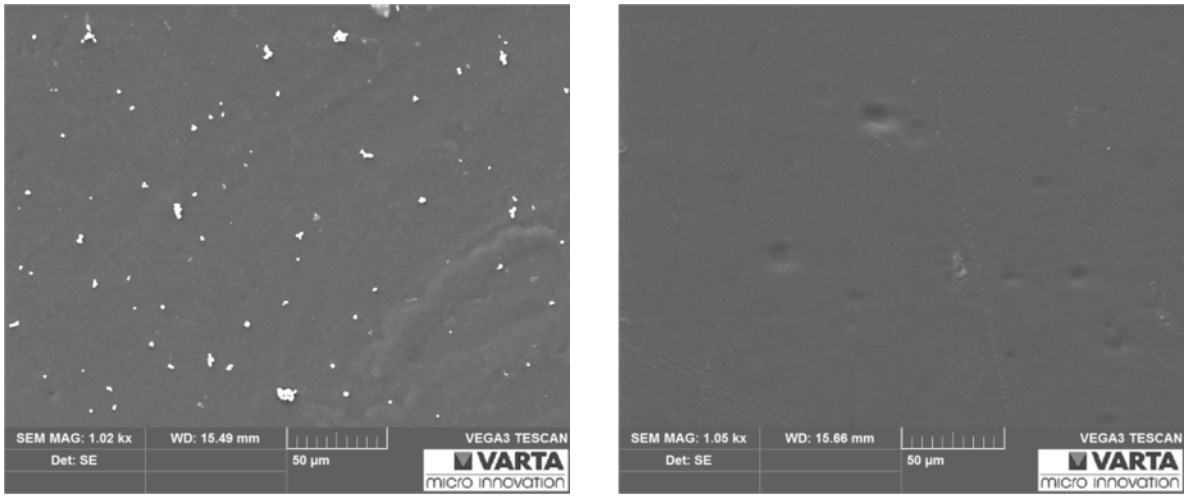

Figure 33: SEM image of the poly(2-oxazoline), blended with benzimidazole (left) and 2-mercaptobenzimidazole (right).

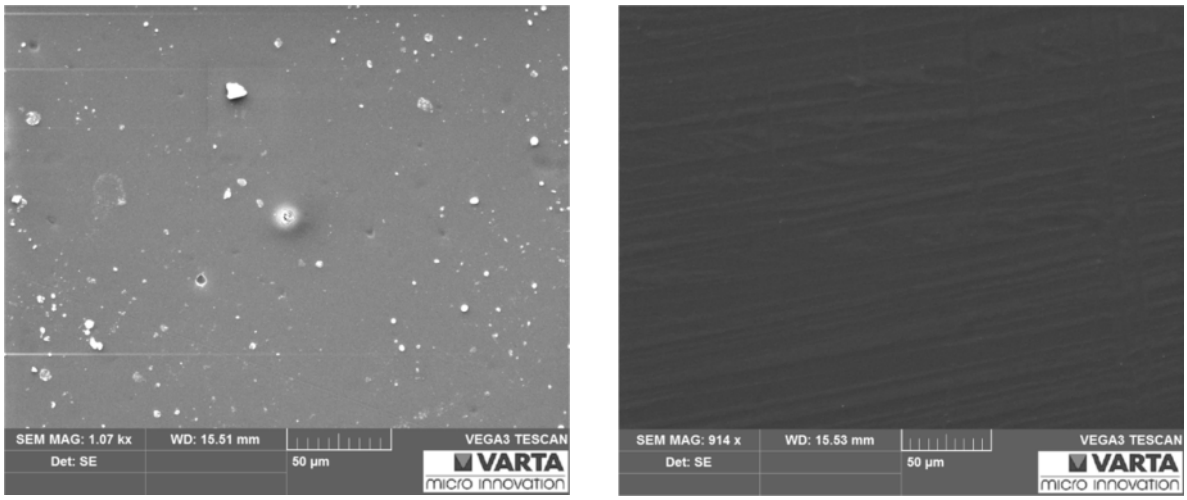

Figure 34: SEM image of the poly(2-oxazoline), blended with *N*-methylurea (left) and *N*-allylurea (right).

It is important to mention that all the measured films appeared homogenous macroscopically. The SEM measurements revealed that the polymer films that were blended with benzimidazole and *N*-methylurea are inhomogeneous. For the *N*-methylurea blend, aggregates with a diameter of up to 10 µm have formed during sample preparation; most aggregates have a diameter of less than 5 µm. The benzimidazole blend contains aggregates with diameters of around 3 µm that tend to agglomerate to formations with up to 10 µm. These aggregates seem to be the additives, which have precipitated during the drying step of the sample preparation.

In comparison, 2-mercaptobenzimidazole and *N*-allylurea do not seem to have precipitated during the sample preparation. The SEM images reveal very homogenous polymer films with these two additives. This clearly indicates a successful covalent embedment of these additives into the poly(2-oxazoline) matrix.

In Table 1, the EDX results of the different poly(2-oxazoline) films are shown. The polymer film compositions only slightly differ. Minor differences might be caused due to the additives; however, they do not affect the composition a lot, as only 5 wt.-% were added to the polymer.

Table 1: SEM-EDX results of the different poly(2-oxazoline) samples.

Poly(2-oxazoline) filled with …	**Carbon [%]**	**Oxygen [%]**	**Sulphur [%]**
Unfilled	78	18	4
Benzimidazole	84	12	5
2-Mercaptobenzimidazole	82	14	4
N-Methylurea	79	17	4
N-Allylurea	80	16	4

The polysiloxane blends have been characterized by SEM-EDX measurements as well. The images are shown in Figure 35 and 36. As already mentioned, during the preparation of the polysiloxane films with 2-mercaptobenzimidazol, the additive precipitated. The SEM images reveal the inhomogeneity of the films, indicating that the covalent embedment was not successful, which correlates very well with the IR spectroscopy results. The non-covalently embedded additives benzimidazole and *N*-methylurea show a similar behavior like in the poly(2-oxazoline) films. Again, the additives had precipitated; the polymer film blended with *N*-allylurea occurs mostly homogenous indicating a successful covalent incorporation of this additive.

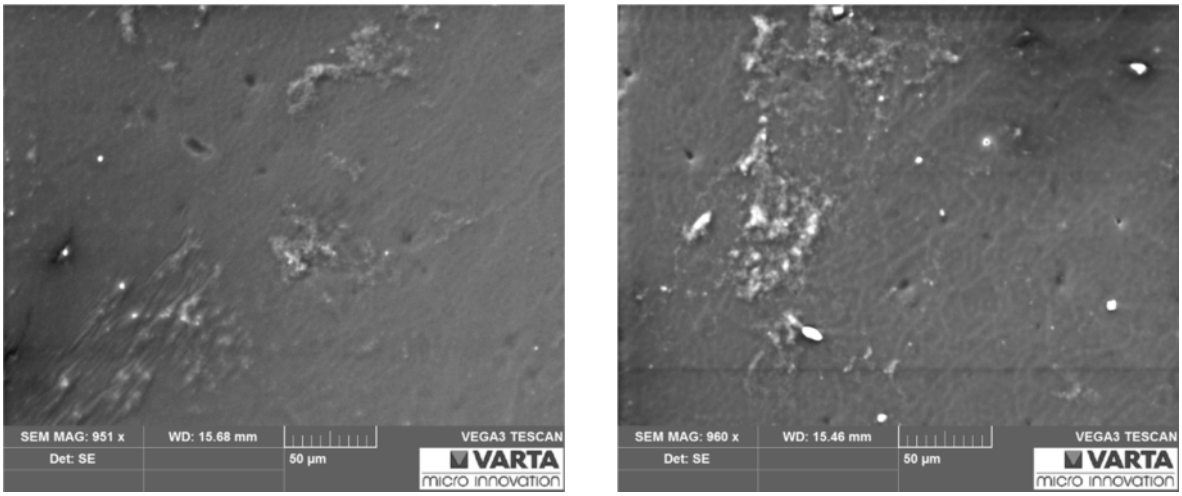

Figure 35: SEM image of the polysiloxane blended with benzimidazole (left) and 2-mercaptobenzimidazole (right).

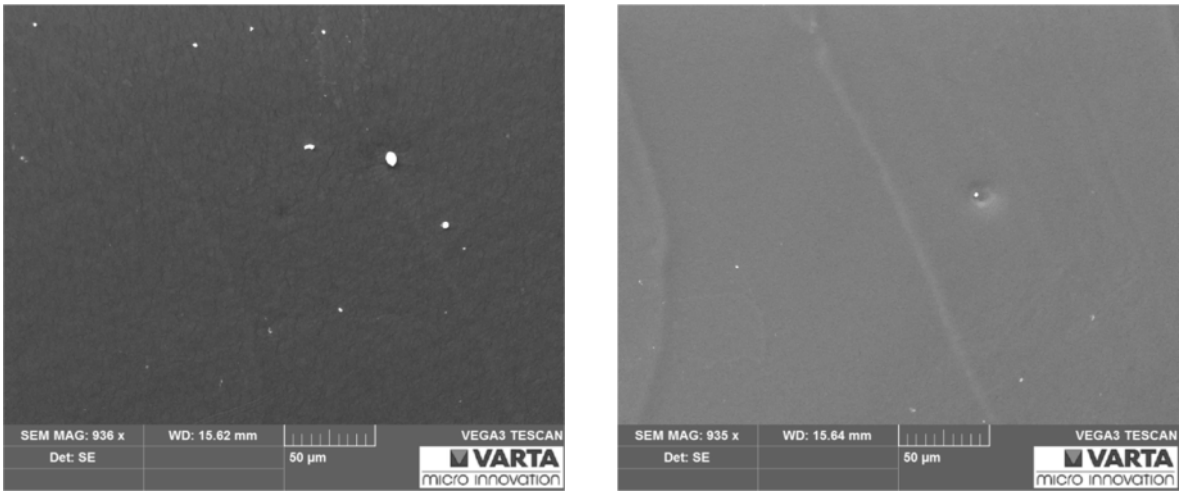

Figure 36: SEM image of the polysiloxane blended with *N*-methylurea (left) and *N*-allylurea (right).

Images with higher magnifications have been recorded as well (Figure 37). For the polymer films blended with benzimidazole and *N*-methylurea, one can clearly see the precipitated aggregates. In comparison, the *N*-allylurea blend seems to be very homogenous even at this highly magnified image. In general, the precipitates seem to have smaller diameter compared to the poly(2-oxazoline) blends.

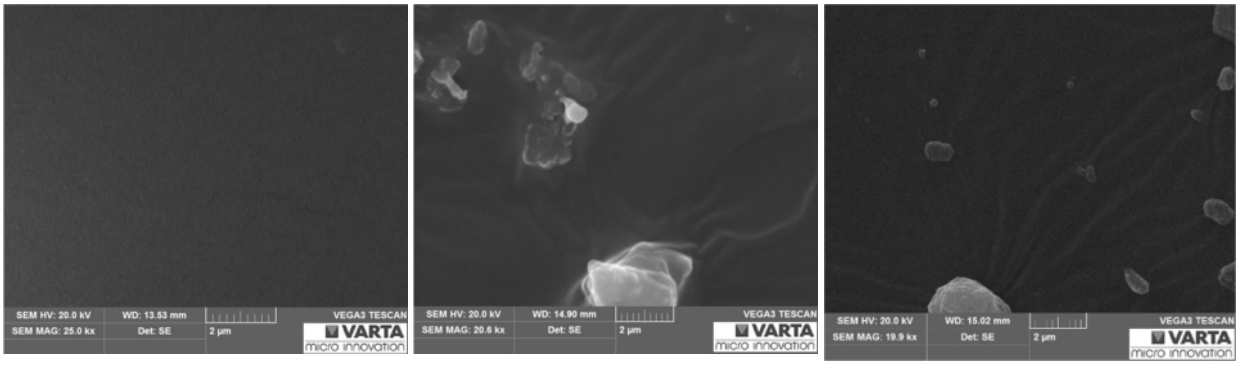

Figure 37: SEM images of polysiloxane samples, blended with (left) *N*-allylurea, (middle) benzimidazole, and (right) *N*-methylurea.

Also, EDX analyses of the polysiloxane blends were performed (Table 2). Throughout the different polysiloxane blends, the compositions vary only marginally. As already mentioned for the poly(2-oxazoline) blends, the additives do not greatly affect the composition, as only 5 wt.-% are incorporated.

Table 2: SEM-EDX results of the different polysiloxane samples.

Polysiloxane filled with …	Carbon [%]	Oxygen [%]	Silicon [%]	Sulphur [%]
unfilled	51	14	15	20
benzimidazole	50	17	16	17
2-mercaptobenzimidazole	51	14	17	18
N-methylurea	51	16	16	17
N-allylurea	50	17	14	19

4.7 TGA and DSC Characterization of the Polymers

Thermal gravimetric analysis and differential scanning calorimetry have been performed in order to characterize the thermal stability of the polymer systems and to determine the glass-transition temperature. The influence of the additives on the thermal properties was investigated (Table 3). In the course of the TGA measurements, a decomposition temperature of 300 °C was observed for the different polysiloxane blends, while it was 230 °C for the different poly(2-oxazoline) blends. The different incorporated additives had no observable influence on the decomposition temperature of the polysiloxane or the poly(2-oxazoline) system. Interestingly, both polymers show a similar T_g of approximately 143 °C. The additives did not influence the glass-transition temperature.

Table 3: Glass-transition temperatures of the polymers and the polymer blends.

Polysiloxane filled with …	**T_g [°C]**	**Poly(2-oxazoline) filled with …**	**T_g [°C]**
unfilled	143	unfilled	144
benzimidazole	145	benzimidazole	143
2-mercaptobenzimidazole	144	2-mercaptobenzimidazole	144
N-methylurea	146	*N*-methylurea	144
N-allylurea	144	*N*-allylurea	143

4.8 Zeta Potential Measurements and Isoelectric Point

With the characterization of the zeta potential at different pH values, the isoelectric point IEP of the polymers and polymer blends was determined. The measurement of the zeta potential was performed in an aqueous 1mM KCl solution and was performed for the polysiloxane films as well as the poly(2-oxazoline) films (Table 4). A great difference between the two polymer systems is observable: The polysiloxane system shows a drastically lowered IEP in comparison to the poly(2-oxazoline) films. As reference value, polypropylene films show an IEP at roughly pH = 4.

Table 4: Isoelectric points IEPs of the polymers and polymer blends.

Polysiloxane filled with …	IEP	Poly(2-oxazoline) filled with …	IEP
unfilled	0.3	unfilled	5.6
benzimidazole	2.0	benzimidazole	4.9
2-mercaptobenzimidazole	2.9	2-mercaptobenzimidazole	5.6
N-methylurea	1.1	*N*-methylurea	5.4
N-allylurea	4.9	*N*-allylurea	7.2

It is important to mention that determining the IEP of the unfilled polysiloxane and the polysiloxane blended with *N*-methylurea, which are at pronouncedly low pH values, could only be accomplished by extrapolation with a third-order polynomial function. In case of the polysiloxane-based specimens, numerous acidic Si-OH groups are present on the surface, which count responsible for the very low IEPs. Only due to blending the polysiloxanes with additives, an increase of the IEPs can be observed: The additives bear amino groups with alkaline properties and, hence, increase the IEP. Especially *N*-allylurea shows an intense impact on the IEP.

The unfilled poly(2-oxazoline)s already have a comparably higher IEP. Consequently, blending with alkaline additives has less impact on the IEP in comparison to the polysiloxanes. Interestingly, blending with benzimidazole even lowers the IEP of the polymer compared to the unfilled poly(2-oxazoline). *N*-allylurea is the only additive that increases the IEP of the poly(2-oxazoline) to an isoelectric point of more than 7.

4.9 Contact Angle Measurements and Surface Energy

Aiming to characterize the polymer films with respect to their polarity and interaction with environmental fluids such as water, contact angle measurements have been performed. By determining the contact angle of different liquids such as water, diiodomethane, and ethylene glycol on a solid substrate, the surface energy of the sample can be calculated. In Table 5, Figure 38 and 39, the measured contact angles are presented. The contact angles for water are reasonably high, indicating that the polymer systems are hydrophobic. Consequently, the values of the contact angles for diiodomethane are lower. The introduction of additives was assumed to lower the contact angles for water, as the additives have a more polar character than

both types of polymers. However, due to (among others) the different film morphologies dependent (among others) on the uniformity of the additive dispersion in the polymer matrix, the additives do not behave in easily-predictable fashion in the two polymer systems. In poly(2-oxazoline), benzimidazole lowers the contact angle, while the contact angle is increased in polysiloxane. 2-Mercaptobenzimidazole and *N*-methylurea show a similar influence on the contact angle with water in both polymers, while *N*-allylurea decreases the contact angle to a higher extent in poly(2-oxazoline) than in polysiloxane.

Table 5: Results of the contact angle measurements on surfaces of the polymers and polymer blends.

Filler	Contact Angle Water [°]	Contact Angle Diiodomethane [°]	Contact Angle Ethylene Glycol
Polysiloxane			
unfilled	**83.6** ± 2.2	**62.1** ± 1.5	**61.2** ± 2.3
benzimidazole	**57.7** ± 0.4	**45.3** ± 0.5	**70.0** ± 5.8
2-mercaptobenzimidazole	**82.1** ± 2.3	**41.6** ± 3.0	**57.3** ± 5.2
***N*-methylurea**	**82.9** ± 2.0	**72.3** ± 2.3	**63.7** ± 1.0
***N*-allylurea**	**69.2** ± 3.1	**54.4** ± 0.8	**63.3** ± 1.6
Poly(2-oxazoline)			
unfilled	**93.4** ± 1.6	**66.5** ± 0.5	**77.5** ± 0.9
benzimidazole	**100.7** ± 7.5	**51.3** ± 1.7	**79.0** ± 1.5
2-mercaptobenzimidazole	**82.1** ± 2.3	**45.5** ± 1.6	**70.9** ± 4.4
***N*-methylurea**	**85.9** ± 1.2	**59.2** ± 0.6	**80.3** ± 1.1
***N*-allylurea**	**49.1** ± 1.3	**47.1** ± 0.1	**53.2** ± 0.5

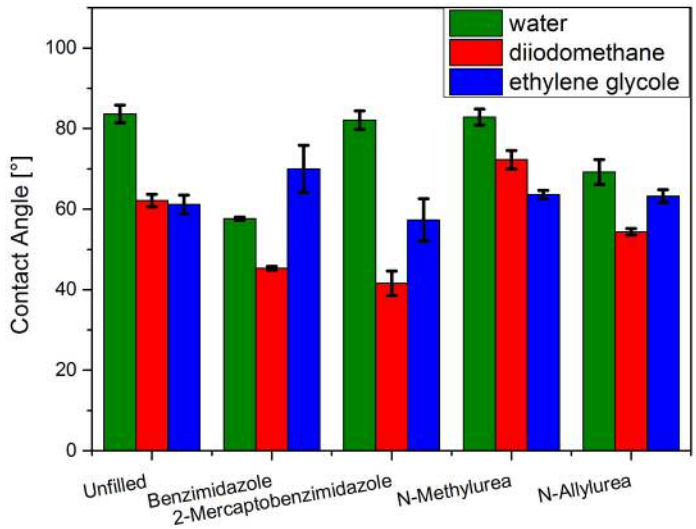

Figure 38: Graphical presentation of the results of the contact angle measurements of the polysiloxane blends.

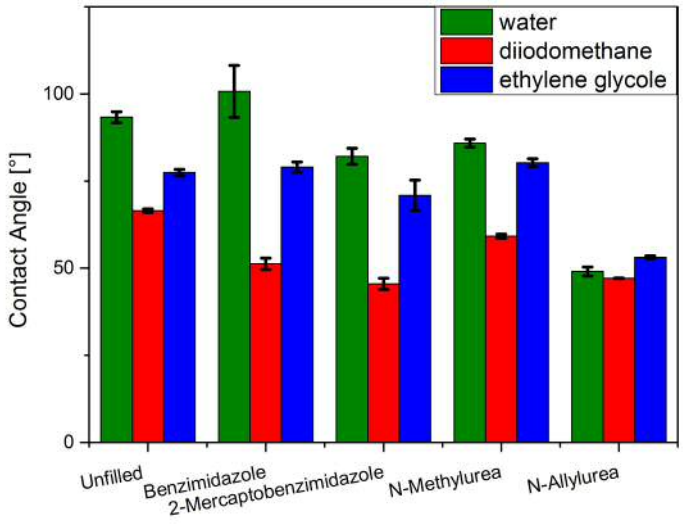

Figure 39: Graphical presentation of the results of the contact angle measurement of the and poly(2-oxazoline) blends.

This behavior might be caused by the morphology of the samples. A descriptive example for the influence of the morphology on the contact angle is the lotus effect. Poly(2-oxazoline)s are capable of forming such nanostructures, especially if 2-nonyl-2-oxazoline is a repetition unit of the polymer chain. Höppener et al. reported nanostructured surfaces of poly(2-oxazoline)s containing 2-nonyl-2-oxazoline units [62]. In Table 6 as well as Figure 40 and 41, the calculated surface energies are presented.

Table 6: Results of the calculated surface energies of the different polymer blends.

	Surface Energy [mN·m^{-1}]	**Dispersive Part [mN·m^{-1}]**	**Polar Part [mN·m^{-1}]**
Polysiloxane			
unfilled	**31.4** ± 2.3	**27.2** ± 1.3	**4.2** ± 1.0
benzimidazole	**51.6** ± 3.7	**36.8** ± 1.8	**14.8** ± 1.9
2-mercaptobenzimidazole	**41.0** ± 4.0	**38.6** ± 2.5	**2.0** ± 1.5
***N*-methylurea**	**26.8** ± 3.8	**20.9** ± 2.3	**5.9** ± 1.5
***N*-allylurea**	**34.2** ± 5.9	**32.0** ± 3.2	**2.6** ± 2.6
Poly(2-oxazoline)			
unfilled	**25.6** ± 2.2	**24.7** ± 1.4	**0.9** ± 0.7
benzimidazole	**33.7** ± 0.1	**33.6** ± 0.1	**0.1** ± 0.0
2-mercaptobenzimidazole	**38.6** ± 5.7	**36.5** ± 3.5	**2.1** ± 2.1
***N*-methylurea**	**30.0** ± 6.4	**28.6** ± 4.4	**1.0** ± 1.0
***N*-allylurea**	**40.0** ± 5.4	**35.8** ± 1.6	**3.9** ± 3.9

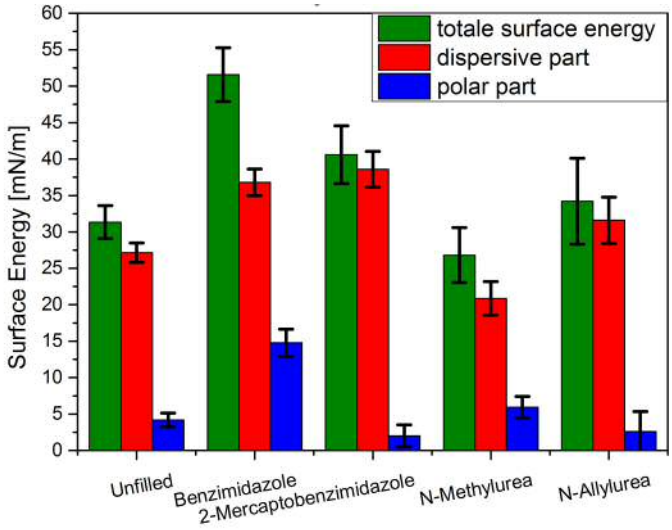

Figure 40: Graphical presentation of the calculated surface energies of the polysiloxane blends.

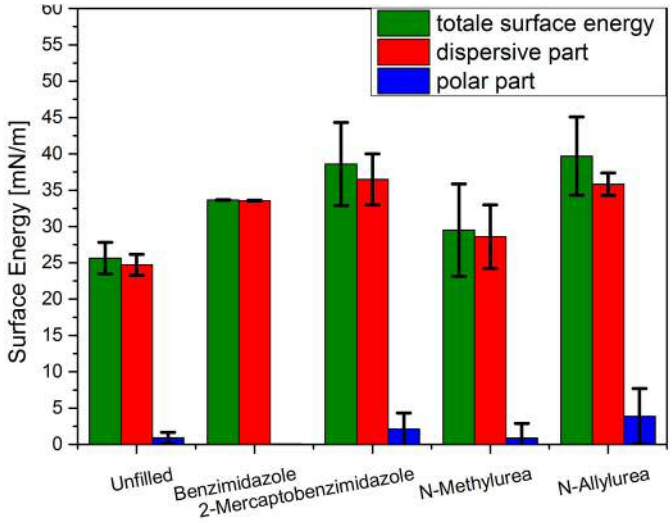

Figure 41: Graphical presentation of the calculated surface energies of the poly(2-oxazoline) blends.

As the contact angles did not show an unambiguously clear trend for the polymer blends in comparison to the unfilled polymers, the calculated surface energies do not provide simple rules-of-thumb either (Table 6, Figure 40 and 41). With dedicated respect to the standard deviations, hardly any alterations of the surface energy can be observed for the poly(2-oxazoline)-based films; in the case of the polysiloxanes, an alteration can be observed only for the imidazoles. This indicates that the additives used do not affect the polarity of the polymer surfaces. A possible reason would be hydrophobic recovery, which may have taken place. Hydrophobic recovery describes the change of the polarity of a polymer surface over time: If polar groups

are present on a surface, they tend to migrate into the bulk to minimize the contact with the very hydrophobic surrounding gaseous medium, namely air. However, as the zeta potential measurements showed an impact of the different additives on the surface properties of the polymer matrices, the major factor influencing the contact angles is presumably the roughness of the polymer samples.

4.10 Impedance Measurements

As the polymer systems are supposed to be suitable for electric applications as insulating materials, impedance measurements have been performed. A schematic of the experimental assembly is shown in Figure 42.

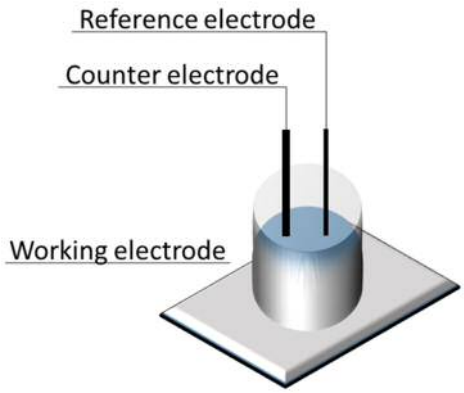

Figure 42: Scheme of the experimental assembly for the impedance measurements.

For the measurement, polymer films were used, which have been applied to an alumina support, which acted as working electrode. Onto the polymer film, a cylinder was placed that was filled with an aqueous 10 wt.-% NaCl solution. A platinum counter electrode and an Ag/Ag^+ reference electrode were placed into the solution. Measurements were performed after application of the NaCl solution onto the polymer films. As the influence of the additives on the ion diffusion was the topic of this work, the polymer films were stored in this assembly, notably in contact with the NaCl solution. Measurements were repeated after 4 h and 24 h.

Values for the resistance of the polymer films at a phase shift close to zero were used for the analysis, aiming to minimize capacitive and inductive influences. The values for the electrical conductivity were calculated from the resistance, the film thickness and the electrode area (Figure 43 and 44).

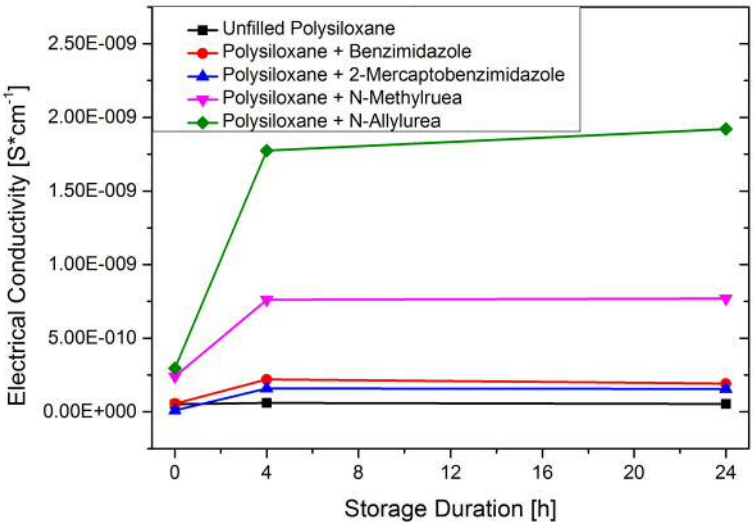

Figure 43: Graphical presentation of the results of the impedance measurements for the polysiloxane blends.

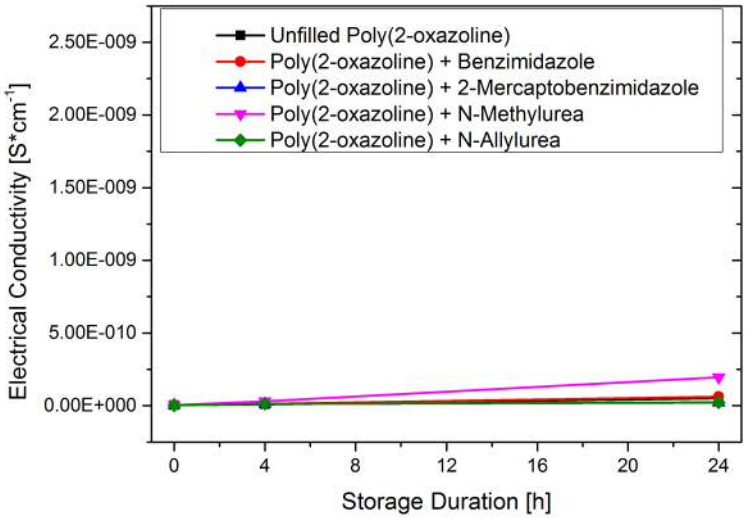

Figure 44: Graphical presentation of the results of the impedance measurements for the poly(2-oxazoline) blends.

The film thickness of the polymer films differed only slightly, with average values of around 150 µm. The electrode area was determined by the cylinder with a value of 15 cm^2. The results for the different polysiloxane blends are shown in comparison to the unfilled polysiloxane. For the blended systems, an initial increase can be observed, afterwards the results become steady. In comparison, blending of the poly(2-oxazoline)s shows a marginal influence only on the electrical conductivity, compared to the polysiloxane blends. In Table 7, the results are summarized.

Table 7: Results of the impedance measurements of the different polymers and polymer blends.

Electrical Conductivity of the Polysiloxanes [S·cm^{-1}]					
Duration [h]	**unfilled**	**benzimidazole**	**2-mercapto-benzimidazole**	***N*-methylurea**	***N*-allylurea**
0	5.08E-11	5.57E-11	9.04E-12	2.39E-10	2.95E-10
4	6.03E-11	2.20E-10	1.59E-10	7.60E-10	1.77E-09
24	5.28E-11	1.92E-10	1.54E-10	7.70E-10	1.92E-09
Electrical Conductivity of the Poly(2-oxazoline)s [S·cm^{-1}]					
Duration [h]	**unfilled**	**benzimidazole**	**2-mercapto-benzimidazole**	***N*-methylurea**	***N*-allylurea**
0	4.75E-12	5.15E-12	3.78E-12	4.79E-12	2.88E-12
4	1.00E-11	1.24E-11	1.24E-11	3.03E-11	1.32E-11
24	5.19E-11	6.26E-11	2.14E-11	1.96E-10	2.26E-11

The results show that initially the unfilled poly(2-oxazoline) is less conducting than the unfilled polysiloxane system. During storage in the electrolyte solution, the difference in the electrical conductivity for these two systems, however, becomes obsolete. An important factor for this behavior is the water uptake: Polysiloxanes are known for their extremely low water uptake. Despite the fact that the poly(2-oxazoline) used in this study contains C_9- and C_{10} side-chains, its water uptake is still higher than that of the polysiloxane.

Aiming to quantify this parameter, a sample of the two polymer systems was weighed, stored in water for 24 h, and weighed again afterwards. The polysiloxane showed a water uptake of 0.4 wt.-%, while the poly(2-oxazoline) gained 1.9 wt.-%.

For the poly(2-oxazoline) blends, a minor change only of the electrical conductivity can be observed (Figure 44). Table 7 reveals that the electrical conductivity increases for the different poly(2-oxazoline) blends over time, but one order of magnitude below the values for the polysiloxane blends. With the exception of the *N*-methylurea blend, this behavior is very similar for the different poly(2-oxazoline) blends and may be mostly due to the water uptake. Analogously, no difference between covalently embedded and simply blended additives can be observed.

Nonetheless, the additives used obviously have an influence on the electrical properties of the polysiloxane blends. *N*-methylurea and especially *N*-allylurea greatly increase the electrical conductivity. Benzimidazole and 2-mercaptobenzimidazole have a similar influence on the polymer system, clearly, however, lower than the other additives. As benzimidazole and 2-mercaptobenzimidazole have very similar

structures, and the covalent embedment of 2-mercaptobenzimidazole was not observed, this similar behavior can be retraced to the films' morphologies.

In general, the influences of the additives are supposed to be due to the formation of complexes. The additives based on urea, as well as the azole-based additives are known to be capable of forming complexes with different ions such as Na^+. Therefore, as sodium ions are present in the electrolyte solution, such complexes can be formed in the blended polymer matrix. Obviously, if a lot of ionic species are present throughout the polymer, the resistivity is lowered, resulting in higher electrical conductivity.

4.11 Diffusion Studies and Characterization

In order to investigate the influence of the formation of these complexes on the ion conductivity, a diffusion study was performed: The polymer films were used as membrane between two compartments (Figure 45).

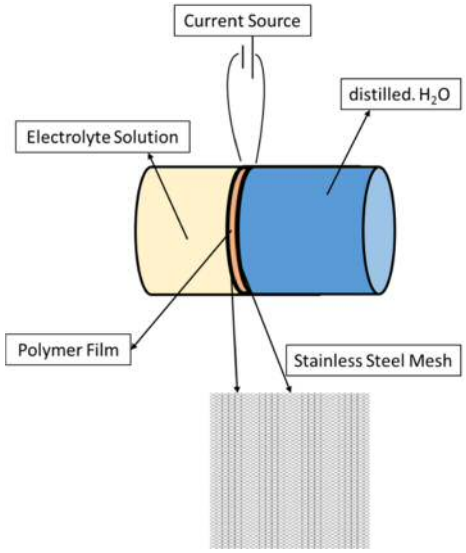

Figure 45: Scheme for the experimental assembly of the ion diffusion experiment.

Each compartment was filled with a volume of 100 mL, separated by the polymer film. As electrolyte solution, a 10 wt.-% aqueous NaOH solution was chosen. Aiming to enhance ion diffusion, an electrical field was applied by connecting a 9 V battery to steel meshes on both sides of the polymer. Those steel meshes were in direct contact to the polymer film. With a film thickness of 150 µm and an applied voltage of

9 V, an electrical field of 60 $kV \cdot m^{-1}$ was established. The experiment was performed for 48 h for each polymer film and each polymer blend. After 24 h and 48 h, a sample of the compartment with the distilled water was taken, and the pH-value was measured. The results are shown in Table 8.

Table 8: Results of the measured pH values during the diffusion experiment of the different polymers and polymer blends.

Polysiloxane					
pH-Value	**unfilled**	**benzimidazole**	**2-mercapto-benzimidazole**	***N*-methylurea**	***N*-allylurea**
after 24 h	6.4	7.2	7.1	7.4	6.7
after 48 h	6.2	7.3	6.8	7.2	7.0
Poly(2-oxazoline)					
pH-Value	**unfilled**	**benzimidazole**	**2-mercapto-benzimidazole**	***N*-methylurea**	***N*-allylurea**
after 24 h	7.6	7.3	7.6	7.7	7.3
after 48 h	7.4	7.2	7.4	7.5	7.4

For the polysiloxane blends, a general increase in the pH value was observed compared to the unfilled polymer. This increase might be due to leaching of the additives from the polymer matrix into the distilled water. For the poly(2-oxazoline)s, on the other hand, no changes can be determined: The pH values of the unfilled polymer as well as the blends do not differ to each other to a distinct extent. In general, the pH-values slightly decrease from 24 h to 48 h, which is supposed to be due to the dissolution of CO_2 from ambient air into the distilled water.

In order to investigate the ion diffusion in more detail, the aqueous samples were analyzed by ICP-OES focusing on their sodium content. Aiming to quantify the measured results, also a blank of distilled water was measured, which was treated equally to the measured aqueous samples. The measured samples had a volume of 10 mL. In Table 9, the results of the ICP-OES analyses are summarized. The blank sample with a value of 2.1 $mg \cdot L^{-1}$ had been subtracted from the results.

Table 9: Results of the measured Na-contents during the diffusion experiment of the different polymer blends.

Polysiloxane					
Na content [mg·L^{-1}]	**unfilled**	**benzimidazole**	**2-mercapto-benzimidazole**	***N*-methylurea**	***N*-allylurea**
after 24 h	3.3	4.1	4.3	3.6	3.3
after 48 h	2.4	5.0	4.7	3.3	3.3
Poly(2-oxazoline)					
Na content [mg·L^{-1}]	**unfilled**	**benzimidazole**	**2-mercapto-benzimidazole**	***N*-methylurea**	***N*-allylurea**
after 24 h	2.9	3.3	3.7	3.3	4.0
after 48 h	2.9	3.4	4.4	3.4	3.4

In general, the measured sodium content of the polymer blends is higher than that of the unfilled polymer. However, the measured sodium content is in the low ppm range, and the samples were prepared under standard laboratory conditions, with present dust particles, which can influence the results. When the sodium ions diffuse through the polymeric system, they also accumulate in the used membrane. Therefore, the amount of sodium present in the polymer was analyzed by ICP-OES as well. The obtained results are shown in Figure 46 and 47 and Table 10. (The sodium content of the unfilled polysiloxane membrane could not yet be determined due to equipment failure during sample preparation.)

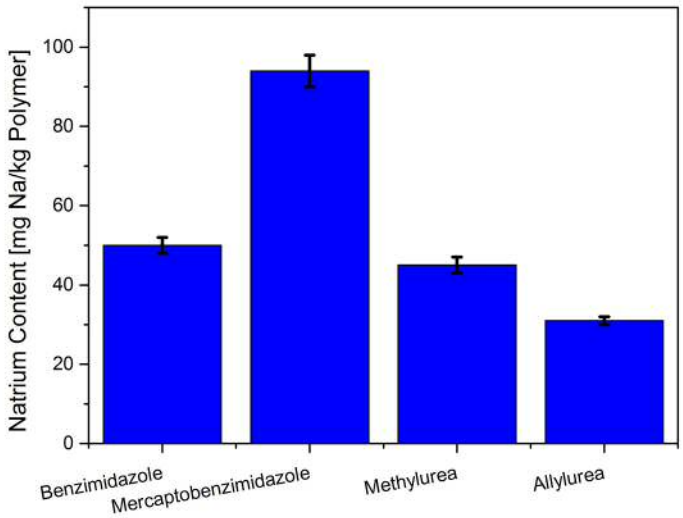

Figure 46: Sodium content of the different used polysiloxane membranes.

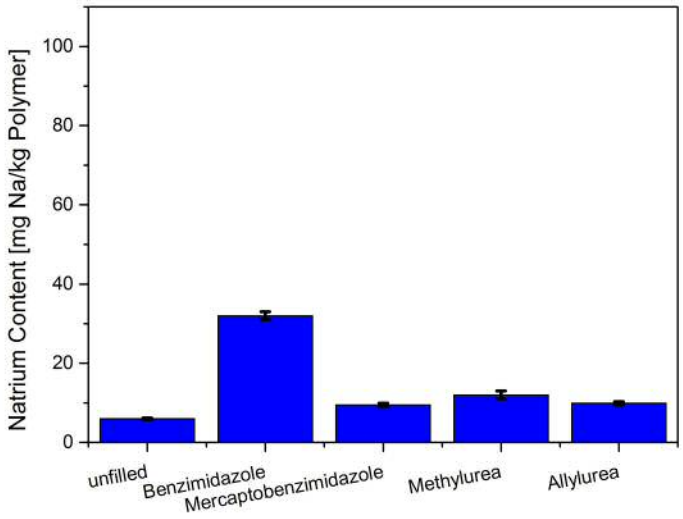

Figure 47: Sodium content of the different poly(2-oxazoline) membranes.

For the polysiloxane blends, the values for the sodium contents are drastically increased in comparison to the different poly(2-oxazoline) membranes. This behavior is in great accordance with the earlier described results of the impedance measurements, where the different poly(2-oxazoline) blends also experienced a comparably low influence.

Table 10: Results from the ICP-OES measurements of the different used blended and unfilled polymer membranes.

Na content in Polysiloxane [ppm]				
unfilled	**benzimidazole**	**2-mercapto-benzimidazole**	***N*-methylurea**	***N*-allylurea**
50 ± 2	94 ± 4	45 ± 2	31 ± 1	50 ± 2
Na content in Poly(2-oxazoline) [ppm]				
unfilled	**benzimidazole**	**2-mercapto-benzimidazole**	***N*-methylurea**	***N*-allylurea**
6 ± 0.2	32 ± 1	9.5 ± 0.4	14 ± 1	9.9 ± 0.4

Interestingly, the polysiloxane blends with *N*-methylurea and *N*-allylurea show a lower sodium content compared to the benzimidazole and 2-mercaptobenzimidazole blends. In comparison, the impedance measurements showed increased electrical conductivity values especially for the polysiloxane blends with the urea-based additives.

5. Conclusions and Outlook

The aim of this work was to investigate the influence of different polar additives on the ion diffusion and ion migration in crosslinked polymer networks. Two different polymer systems, one based on polysiloxanes and one based on poly(2-oxazoline)s were chosen and blended with two different additive classes, one based on benzimidazole, and the second class based on urea. For both additive classes, also covalent embedment was part of the investigations.

The poly(2-oxazoline) was a copolymer based on 2-dec-9'-enyl-2-oxazoline and 2-nonyl-2-oxazoline. It was chosen because of its hydrophobic character due to the long olefinic side-chains. The synthesis of these two monomers was performed according to the Henkel patent [42], where the corresponding fatty acid reacts with ethanolamine to yield the 2-oxazoline. As catalyst, the titanium catalyst $Ti(BuO)_4$ was used. The copolymerization was performed via microwave-assisted cationic ring-opening polymerization in acetonitrile as solvent. For the initiation of this polymerization, methyl tosylate was used, yielding a polymer with a polymerization degree of 100 with 20 units of 2-dec-9'-enyl-2-oxazoline and 80 units of 2-nonyl-2-oxazoline. The polymerization is pseudo-living and, therefore, yields polymers and copolymers with a narrow molecular weight distribution. The crosslinking of this polymer was performed via the UV induced thiol-ene click reaction. The photoinitiator Lucirin TPO-L and 2,2′-(ethylenedioxy)diethanethiol as crosslinker were used to obtain a highly crosslinked polymer system.

The second used polymer matrix was based on 1,3-divinyltetramethyldisiloxane, which was cured via the UV induced thiol-ene click reaction with trimethylolpropane tris(3-mercaptopropionate) and 2,2′-(ethylenedioxy) diethanethiol in a ratio of 8:2. Also this polymer system, like most polysiloxanes, shows hydrophobic character.

From these two polymer systems, thin films with a thickness of approx. 150 µm were produced. Also, polymer blends with the selected additives were prepared. The covalent embedment of the additives was performed via the thiol-ene click reaction during the curing step of the polymers.

Different characterization techniques were used to investigate the properties of these polymer films. IR spectroscopy clearly showed the successful covalent embedment of suitable additives into the polymer matrix by the thiol-ene click-reaction. Notably, the

covalent attachment of mecaptobenzimidazole into the polysiloxane network could not be accomplished quantitatively, most likely due to the tautomeric equilibrium that lowers the reactivity of that additive.

Additionally, the covalent embedment was verified by SEM images (Figure 48). The not-covalently embedded *N*-methylurea precipitated during sample preparation, whereas the covalently embedded *N*-allylurea did not precipitate and is homogenously distributed throughout the polymer film. Hence, this covalent embedment can have a great impact, as the additive is tightly bond and, therefore, cannot migrate through the system or even be washed out of the polymer matrix.

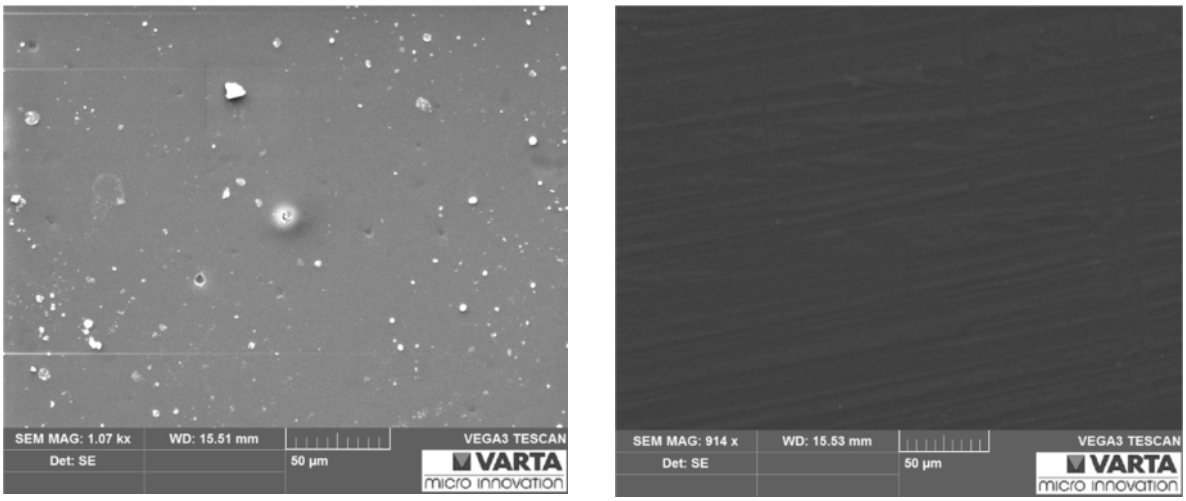

Figure 48: SEM images of the poly(2-oxazoline)s, blended with (left) *N*-methylurea and (right) *N*-allylurea.

Thermogravimetric analysis and differential scanning calorimetry were performed to investigate the thermal stability of the polymer systems as well as the polymer blends and to determine their glass-transition temperatures. It was concluded that the additives affect these properties to a very narrow extent only.

In order to investigate the influence of the additives on the surface of the polymer systems, zeta potential measurements as well as contact angle measurements were performed. For the zeta potential measurements, it was observable that the additives tend to shift the isoelectric point to a higher pH value, as the additives contain amine functionalities. From the contact angles, the surface energy of the polymer systems and blends had been calculated. From these investigations, no clear trend could be observed, likely due to the surface roughness of the polymer matrices.

As the unfilled polymer films and blended polymer films are supposed to have insulating properties, impedance measurements were performed to investigate their electrical conductivity (Figure 49). An aqueous NaCl solution was cast onto the polymer films. The films were measured immediately and after 4 and 24 h to investigate the influence of the additives.

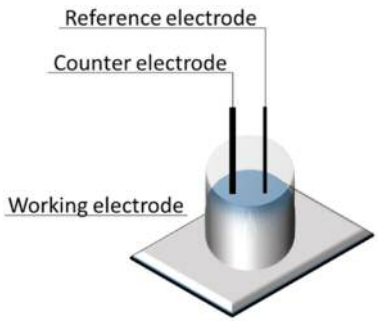

Figure 49: Scheme of the experiment assembly for the impedance measurements.

In particular the properties of the polysiloxane blends were affected by the additives (Figure 50). The additives based on urea enhanced the electrical conductivity significantly. The poly(2-oxazoline) blends were affected only marginally.

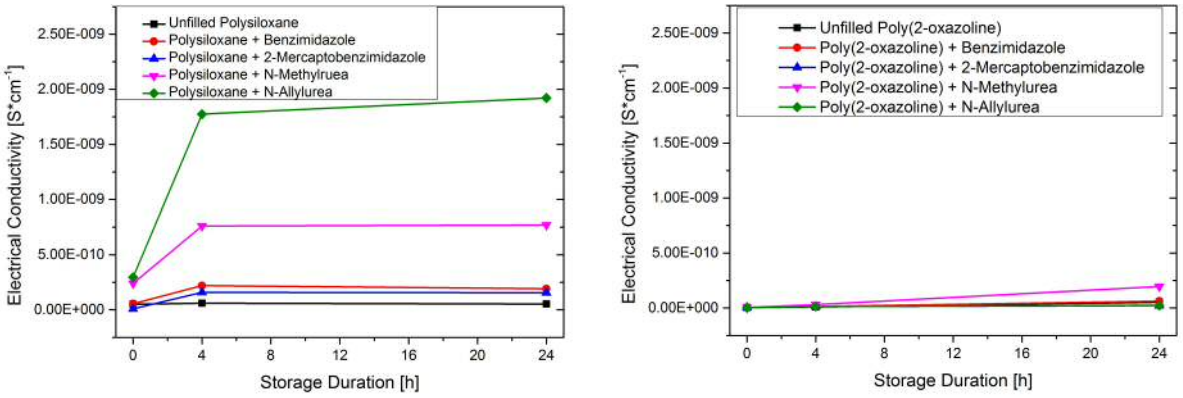

Figure 50: Graphical presentation of the results of the impedance measurements for the polysiloxane blends (left) and the poly(2-oxazoline) blends (right).

In order to further investigate the diffusion behavior of the polymer films, diffusion experiments were performed, in which the polymer films acted as membrane between a compartment filled with distilled water and a compartment filled with an aqueous NaCl solution. The ion migration was enhanced by applying an electrical field using a 9 V battery, which was connected to a steel mesh on both sides of the membrane (Figure 51).

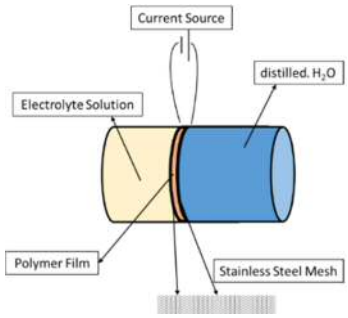

Figure 51: Scheme for the experimental assembly of the ion diffusion experiment.

In order to quantify the ion diffusion and ion migration, ICP-OES measurements were performed. Therefore, samples of the compartment with distilled water, as well as of the polymer films were analyzed with respect to their Na content. Especially the ICP-OES measurements of the polymer samples showed remarkable results (Figure 52).

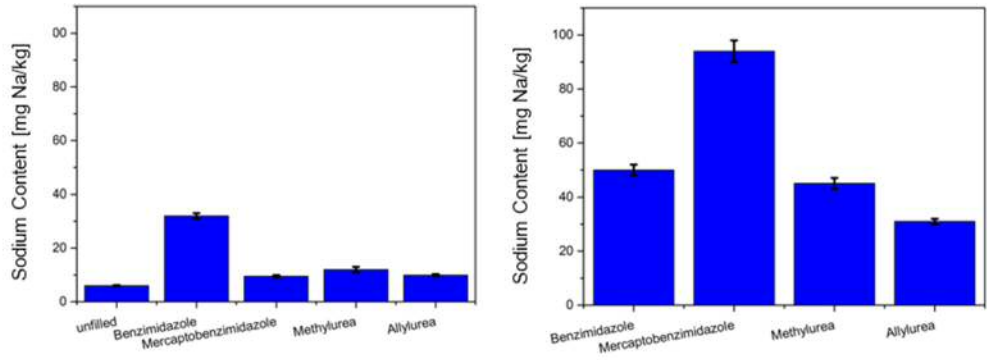

Figure 52: Sodium contents of the different polymer membranes and blended polymer membranes, determined by ICP-OES. Left: Poly(2-oxazoline)s; right: polysiloxanes.

The polysiloxane membranes showed a great increase of the sodium content compared to the poly(2-oxazoline) films. These results are in great accordance with the observed results from the impedance measurements, where the additives have a much higher impact on the polysiloxane matrix as well.

At the current state-of knowledge, it may be argued that the polysiloxane filled with 2-mercaptobenzimidazole shows the highest sodium ion uptake. It must be stated in critical fashion, nonetheless, that the covalent attachment of that ligand had not yet been accomplished in quantitative fashion, which is the subject of on-going research. For further investigations, the use of electrolyte solutions containing copper would be very interesting for the impedance measurements as well as for the diffusion studies.

6. Abstract

In this work, the influence of different additives on the diffusion and migration behavior of ions in different polymer matrices was investigated. Therefore, polymer films were prepared, which were blended with polar additives capable of forming complexes with metal ions like sodium. As polymer matrices, a copolymer based on 2-oxazolines with hydrophobic side-chains, and a polymer based on siloxane were chosen. From these two materials, dense polymer networks were produced via the UV induced thiol-ene click-reaction. During the curing step, additives with dedicated functionality were covalently embedded into the polymer matrix; the influence of the covalent attachment on the material properties, in particular ion uptake was investigated. The covalent attachment to the polymer matrices was confirmed by IR spectroscopy and SEM-EDX measurements

The surfaces of the polymer films were analyzed by contact angle measurements and zeta potential measurements. Due to the given roughness of the different polymer substrates, no clear trend could be observed. However, the influence of the additives on the polymer surface was confirmed by zeta potential measurements. The isoelectric point was determined, which shifted towards higher pH values due to the presence of additives that contain amino functionalities.

In order to investigate the ion diffusion and ion migration behavior of the polymers, impedance spectroscopy using an aqueous NaCl electrolyte solution in direct contact with the polymer film was performed. Especially for the polysiloxane that was blended with urea-based additives, a great increase in the electrical conductivity was observed.

Additionally, the polymer films were used as membrane for 48 h between two compartments with differing NaCl concentrations in order to investigate the ion migration behavior. With ICP-OES measurements, the sodium content of the polymer films was determined. The polysiloxane blends showed a great increase of the sodium content, while the poly(2-oxazoline) membranes only showed a slight increase in the sodium content.

7. Kurzfassung

In dieser Arbeit wurde der Einfluss verschiedener Additive auf das Diffusions- und Migrationsverhalten von Ionen in verschiedenen Polymersystemen untersucht. Verschiedene Polymerfilme wurden hergestellt, welchen geeignete polare Additive zugesetzt wurden, die verschiedene Metallionen wie Natrium komplexieren können. Als Polymermatrix wurden ein Copolymer auf Basis von 2-Oxazolinen mit hydrophoben Seitenketten und ein Polymer auf Siloxanbasis ausgewählt. Mittels der UV-induzierten Thiol-En Klick-Reaktion konnten dichte Polymernetzwerke hergestellt werden. Während dieses Aushärtungsschritts wurden ausgewählte Additive kovalent in die Polymermatrix eingebettet, um ein mögliches unterschiedliches Verhalten zu untersuchen. Dieser kovalente Einbau in das Polymernetzwerk konnte mittels IR-Spektroskopie und SEM-EDX-Messungen bestätigt werden.

Die Oberfläche der hergestellten Polymerfilme wurde durch Kontaktwinkelmessungen und Zeta-Potential-Messungen analysiert. Durch die raue Oberflächenmorphologie der Polymerproben konnte durch die Kontaktwinkelmessungen kein Einfluss der verschiedenen Additive ermittelt werden. Jedoch konnten Zeta-Potential-Messungen den Einfluss der verschiedenen Additive auf die Oberflächeneigenschaften der Polymerproben bestätigen. Der isoelektrische Punkt wurde bestimmt und durch die Gegenwart der verschiedenen Additive zu höheren pH-Werten hin verschoben, da diese Aminofunktionalitäten enthalten.

Um das Ionendiffusions- und Ionenmigrationsverhalten dieser verschiedenen Polymere zu untersuchen, wurde Impedanzspektroskopie unter Verwendung einer NaCl-Elektrolytlösung in direktem Kontakt mit den Polymerfilmen durchgeführt. Insbesondere bei den Polysiloxanfilmen, welche mit den auf urea-basierenden Additiven geblendet wurden, konnte ein starker Anstieg der elektrischen Leitfähigkeit beobachtet werden.

Zusätzlich wurden die Polymerfilme für 48 h als Membran in einer Migrationszelle mit unterschiedlichen NaCl-Konzentrationen verwendet, um das Ionenmigrationsverhalten zu untersuchen. Mittels ICP-OES wurde anschließend der Natrium-Gehalt der verwendeten Membranen bestimmt. Auch hier zeigten besonders die geblendeten Polysiloxanfilme einen erhöhten Natrium-Anteil im Vergleich zu den Poly(2-oxazolin)-Membranen.

8. Materials and Methods

8.1 Used Chemicals

Suppliers of the commercially available chemicals are summarized in Table 11. All chemicals were used as received, with the exception of methyl tosylate that was distilled prior to use.

Table 11: List of the chemicals used.

Chemical	Purity	Supplier
1-methoxy-2-propanol	>99%	Carl Roth
1,3-divinyltetramethyldisiloxane	98%	ABCR
2-aminoethanol	98%	Sigma-Aldrich
2-mercaptobenzimidazole	98%	Sigma-Aldrich
2,2′-(ethylenedioxy)diethanethiol	95%	Sigma-Aldrich
2,4,6-trimethylbenzoylphenyl-phosphinic acid ethyl ester	95%	ABCR
acetonitrile	99.5%	Carl Roth, Austria
benzimidazole	98%	Sigma-Aldrich
chloroform	99.2%	AnalaR Normpur
decanoic acid	98%	Sigma-Aldrich
methyl tosylate	98%	Sigma-Aldrich
N-allylurea	95%	Sigma-Aldrich
N-methylurea	97%	Sigma-Aldrich
titanium(IV)butoxide	99%	Sigma-Aldrich
trimethylolpropane tris(3-mercaptopropionate)	95%	Sigma-Aldrich
undec-10-enoic acid	97%	Sigma-Aldrich

8.2 Analytical Methods

NMR measurements. A Bruker Advance III 300 MHz spectrometer was used for the NMR analyses. The measurements were performed using deuterated chloroform $CDCl_3$ as solvent. The solvent peaks at 7.26 ppm (^{1}H-NMR) and 77.0 ppm (^{13}C-NMR) were used as reference.

IR measurements. A Bruker Alpha Fourier-Transform Infrared Spectrometer with ATR support was used for the IR spectroscopy measurements. For every measurement, the background was recorded in advance. 48 scans were performed for every analysis in the range of 400-4000 cm^{-1}.

Microwave-assisted synthesis. For the microwave-assisted polymerization reactions, a Biotage Initiator 8 microwave reactor with auto sampler and internal infrared sensor for the monitoring of reaction temperatures was used.

Gel permeation chromatography. For the determination of the average molar mass of the polymers, GPC analyses were performed with a Shimadzu SEC system, an LC-20AD pump and a RID202A refractive index detector. As solvent a mixture of $CHCl_3$/Et_3N/^{iso}PrOH = 94/4/2 was used with a flow of 1 $mL \cdot min^{-1}$.

Differential scanning calorimetry. The DSC analyses were performed with a DSC 8500 from Perkin Elmer with 20 $K \cdot min^{-1}$ as heating rate under nitrogen atmosphere.

UV-induced crosslinking. An EFOS Novacure UV Hg/Xe Lamp of EXFO was used for curing the polymeric systems. The distance between the surface of the reaction mixture and the UV lamp was set to 15 cm. The samples were irradiated with UV light at 6 $W \cdot cm^{-2}$.

Contact angle measurements. For the contact angle measurements, water, diiodomethane and ethylene glycol were used as test liquids. The DSA 100 from Krüss was used for the measurements.

Zeta potential measurements. The zeta potential was measured using the SurPASS Electrokinetic Analyzer and the EKA ElectroKinetic Analyzer from Anton Paar.

SEM-EDX measurements. The measurements were performed using a Tescan Vega 3 scanning electron microscope with an energy-dispersive X-ray spectrometer EDX Oxford Instruments INKAxact. The samples were measured using a voltage of 20 kV.

Impedance measurements. For the impedance measurements, the samples were put onto an alumina support, which also acted as working electrode. As reference, an Ag/Ag^+ electrode was used; a platinum electrode was used as counter electrode. Counter and reference electrode were contacted to the polymer film via an aqueous 10 wt.-% NaCl solution.

Diffusion experiments. For the ionic diffusion experiments, the polymer films were used as a membrane separating two compartments. One compartment was filled with 100 mL of distilled water, and the second was filled with 100 mL of aqueous NaOH solution. An electric field was applied, using a metal mesh on both sides of the membrane, which was connected to a 9 V battery. The pH value was measured after 24 and 48 h. The experiment lasted for 48 h in total.

8.3 Synthesis of 2-Dec-9'-enyl-2-oxazoline (Dec$^=$Ox)

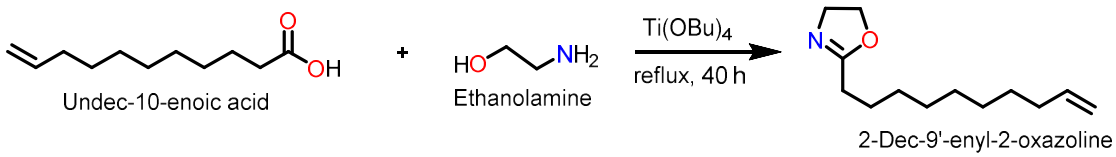

Figure 53: Reaction scheme for the synthesis of 2-dec-9'-enyl-2-oxazoline.

The synthesis of 2-dec-9'-enyl-oxazoline was performed according to the Henkel patent [42]. Undec-10-enoic acid (150 mL; 136.8 g; 0.742 mole; 1 eq.) and ethanolamine (70 mL; 70.82 g; 1.16 mole; 1.56 eq.) were placed in a 500 mL flask. Titanium(IV)-butoxide (1.3 mL; 1.3 g; 3.82 mmole; 0.0051 eq.) was added, and the reaction mixture was heated to 140 °C under stirring. After 20 h and 24 h under reflux, another portion of titanium(IV)-butoxide (1.3 mL; 1.3 g; 3.82 mmole; 0.0051 eq.) was added. The reaction was again stirred overnight. Afterwards, the condenser was removed, and the reaction was stirred at 140 °C for another 12 h. For purification, the product was distilled under reduced pressure (180 °C, <4 mbar). The obtained yellowish product was further purified via column chromatography on silica with chloroform as eluent, yielding the final product as a colorless oily liquid (68.1%, 105.50 g).

^{1}H NMR (300 MHz, $CDCl_3$): δ = 5.77 (m, 1H), 5.04-4.82 (m, 2H), 4.18 (t, $^{3}J_{H,H}$ = 9.4 Hz, 2H), 3.78 (t, $^{3}J_{H,H}$ = 9.3 Hz, 2H), 2.23 (t, $^{3}J_{H,H}$ = 7.5 Hz, 2H), 2.00 (d, $^{3}J_{H,H}$ = 6.7 Hz, 2H), 1.65-1.52 (m, 2H), 1.27 (s, 10H).

^{13}C NMR (75 MHz, $CDCl_3$): δ = 168.7, 139.2, 114.2, 77.6, 77.2, 76.7, 67.2, 54.5, 33.9, 29.4, 29.3, 29.1, 29.0, 28.1, 26.0.

IR (ATR): ν (cm^{-1}) = 2924, 2853, 1667, 1461, 1432, 1361, 1227, 1167, 986, 952, 907.

8.4 Synthesis of 2-Nonyl-2-oxazoline (NonOx)

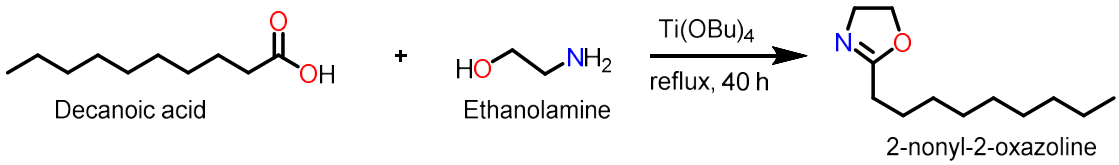

Figure 54: Reaction scheme for the synthesis of 2-nonyl-2-oxazoline.

The synthesis of 2-nonyl-2-oxazoline was performed according to the Henkel patent [42]. Decanoic acid (150 mL; 134.0 g; 0.778 mole, 1 eq.) and ethanolamine (70 mL; 70.82 g; 1.16 mole; 1.49 eq.) were placed in a 500 mL flask. Titanium(IV)-butoxide (1.3 mL; 1.3 g; 3.82 mmole; 0.0049 eq.) was added, and the reaction mixture was heated to 160 °C under stirring. After 20 h and 24 h under reflux, another portion of titanium(IV)-butoxide (1.3 mL; 1.3 g; 3.82 mmol; 0.0051 eq.) was added. The reaction was again stirred overnight. Afterwards, the condenser was removed, and the reaction was stirred at 160 °C for another 12 h. For purification, the product was distilled under reduced pressure (180 °C, <4 mbar). The obtained yellowish product was further purified via column chromatography on silica with chloroform as eluent, yielding the final product as a colorless oily liquid (53.3%, 80.92 g).

^{1}H NMR (300 MHz, $CDCl_3$): δ = 4.20 (t, $^{3}J_{H,H}$ = 9.4 Hz, 2H), 3.80 (t, $^{3}J_{H,H}$ = 9.4 Hz, 2H), 2.25 (t, 7.6 Hz, 2H), 1.67-1.53 (m, 2H), 1.25 (s, 12H), 0.86 (t, 3H).

^{13}C NMR (75 MHz, $CDCl_3$): δ = 168.8, 67.2, 54.5, 32.0, 29.5, 29.4, 28.1, 26.1, 22.8, 14.2.

IR (ATR): ν (cm^{-1}) = 2923, 2853, 1668, 1464, 1362, 1231, 1165, 985, 949, 908, 754.

8.5 Synthesis of Poly(2-nonyl-2-oxazoline)-*stat*-poly(2-dec-9'-enyl-2-oxazoline)

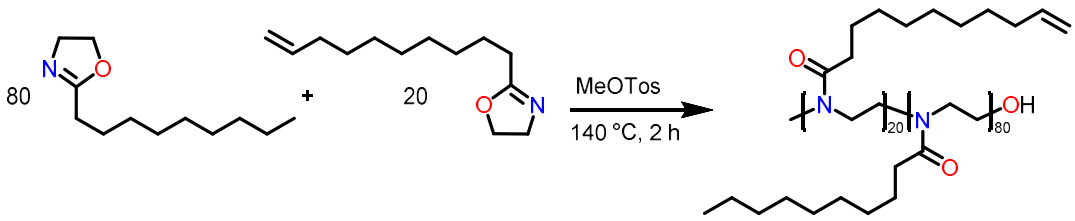

Figure 55: Reaction scheme for the synthesis of poly(2-nonyl-2-oxazoline)-*stat*-poly(2-dec-9'-enyl-2-oxazoline).

The synthesis of poly(2-nonyl-2-oxazoline)-*stat*-poly(2-dec-9'-enyl-2-oxazoline) was performed in the Biotage Initiator 8 microwave reactor. Dec$^{=}$Ox (0.566 g; 2.73 mmole, 1.0 eq.), NonOx (2.139 g; 10.95 mmole; 4.0 eq.), methyl tosylate (25.1 mg; 0.135 mmole; 0.05 eq.) and 2.5 mL acetonitrile were transferred into a microwave vial. The vial was equipped with a stirring bar, crimped, and placed in the auto sampler of the microwave. The microwave was set to operate at 140 °C for 2 h. The adsorption level was set to medium. The product was obtained as a white solid and dried at the rotary evaporator. The final product was obtained as a white powder (> 99%; 2.72 g).

^{1}H NMR (300 MHz, $CDCl_3$): δ = 5.81-5.63 (m, 4H), 4.97-4.79 (m, 8H), 4.06 (s, 2H), 3.49 (d, 80H), 2.80-2.42 (m, 8H), 2.23 (d, 40H), 1.97 (d, 11H), 1.53 (s, 45H), 1.20 (s, 240H), 0.80 (d, 49H).

^{13}C NMR (75 MHz, $CDCl_3$): δ = 173.9, 173.1, 139.0, 125.7, 114.1, 45.1, 36.6, 33.7, 32.8, 31.9, 29.5, 29.3, 28.9, 25.4, 25.2, 22.6, 14.1.

IR (ATR): ν (cm^{-1}) = 2919, 2851, 1639, 1461, 1430, 1181, 1160, 909, 772, 721.

GPC: M_n = 10.3 kDa; M_w = 13.5 kDa; M_w/M_n = 1.31.

8.6 Preparation of the Polymer Films

8.6.1 Crosslinked Polysiloxane Films

1,3-Divinyltetramethyldisiloxane (0.77 g; 4.1 mmol), a mixture of 2,2′-(ethylenedioxy) diethanethiol (0.2 g; 1.1 mmol) and trimethylolpropane tris(3-mercaptopropionate) (0.8 g; 2.0 mmol), as wellas the photoinitiator 2,4,6-trimethylbenzoylphenylphosphinic acid ethyl ester (0.1 g; 0.3 mmol) were dissolved in 1.5 mL of 1-methoxy-2-propanol. After mixing in the ultrasonic bath for 15 min, the liquid reaction mixture was applied onto a flat PET support and distributed to form a thin liquid film. For the crosslinking reaction, the liquid was irradiated with UV light (254 nm, 6 $W \cdot cm^{-2}$) for 30 s. Afterwards, the solid polymer films were lifted off the PET support and irradiated for another 5 min. In order to remove the solvent 1-methoxy-2-propanol, the polymer films were dried at 80 °C for 48 h.

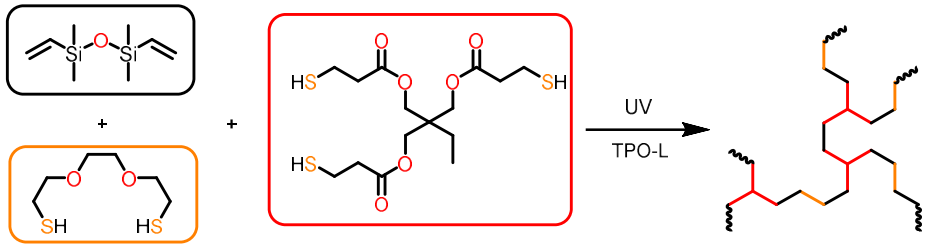

Figure 56: Reaction scheme for the preparation of highly crosslinked polysiloxane networks.

8.6.2 Crosslinked Poly(2-oxazoline) Films

Poly(2-nonyl-2-oxazoline)-*stat*-poly(2-dec-9'-enyl-2-oxazoline) (0.50 g; 0.025 mmol), 2,2′-(ethylenedioxy) diethanethiol (0.046 g; 0.25 mmol) and 2,4,6-trimethylbenzoyl-phenylphosphinic acid ethyl ester (0.1 g; 0.3 mmole) were dissolved in a mixture of 1 mL of 1-methoxy-2-propanol and 1 mL of toluene. After mixing in the ultrasonic bath for 15 min, the liquid reaction mixture was applied onto a flat PET support and distributed to form a thin liquid film. For the crosslinking reaction, the liquid was irradiated with UV light (254 nm, 6 $W \cdot cm^{-2}$) for 30 s. The solid polymer films were lifted off the PET support and irradiated for another 5 min. In order to remove the solvents, the polymer films were dried at 80 °C for 48 h.

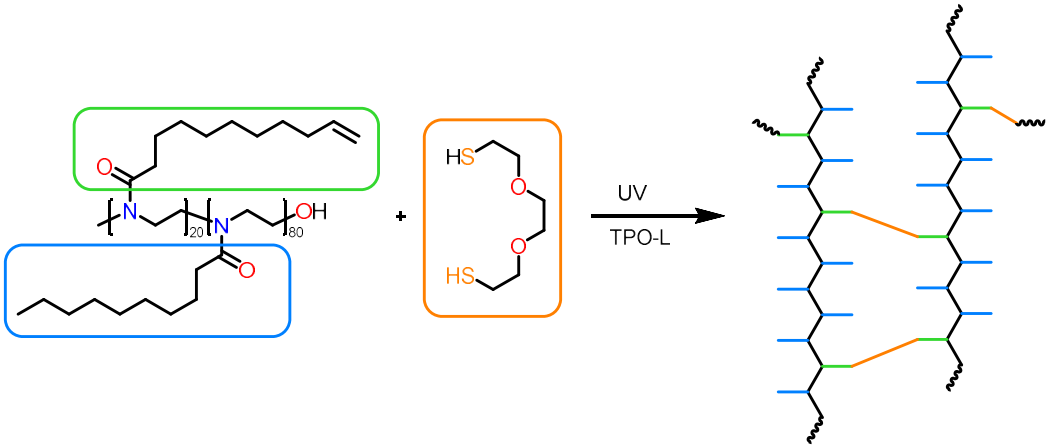

Figure 57: Reaction scheme for the preparation of highly crosslinked poly-2-oxazoline networks.

8.6.3 Incorporation of Additives into the Polymer Films

Additionally, different additives were added to the polymeric systems:

- benzimidazole
- 2-mercaptobenzimidazole
- *N*-methylurea
- *N*-allylurea

The preparation of polymer films containing these additives was performed as described hereinabove. As 2-mercaptobenzimidazole and *N*-allylurea were covalently embedded in the polymer matrix, the amounts of 2,2′-(ethylenedioxy) diethanethiol and trimethylolpropane tris(3-mercaptopropionate) were adapted to the amounts of double bonds and thiol functionalities of the additives, respectively. Benzimidazole and *N*-methylurea were incorporated into the polymer matrix by blending without covalent attachment. For the preparation of these polymer films, 5 wt.-% of the corresponding additive was dissolved together with the other reactants. As these additives are solids, complete solvation is crucial. Therefore, the reaction mixtures were heated to 60 °C under stirring for 5 min and afterwards sonicated for 15 min.

9. Appendix

9.1 List of Figures

9.2 List of Tables

10. Literature

[1] Moore, G. E.: Cramming more components onto integrated circuits. *Electronics* **1965**, *38*, 114. DOI:10.1109/N-SSC.2006.4785860

[2] Tanaka, S. I., Kashahara, K., Shimawaki, H., & Honjo, K.: Stress current behavior of InAlAs/InGaAs and AlGaAs/GaAs HBT's with polyimide passivation. *IEEE Electron. Device Letters* **1992,** *13*, 560-562. DOI: 10.1109/55.192839

[3] Hood, A., Delaunay, P. Y., Hoffman, D., Nguyen, B. M., Wei, Y., Razeghi, M., Nathan, V.: Near bulk-limited R0A of long-wavelength infrared type-II In As⁄ Ga Sb superlattice photodiodes with polyimide surface passivation. *Appl. Physics Lett.* **2009**, *90*, 233513. DOI: 10.1063/1.2747172

[4] Obreja, V. V.: On the leakage current of present-day manufactured semiconductor junctions. *Solid-State Electron.* **2000**, *44*, 49-57. DOI: 10.1016/S0038-1101(99)00208-7

[5] Meynen, H., Bulcke, M. V., Gonzalez, M., Harkness, B., Gardner, G., Sudbury-Holtschlag, J., Vandevelde, C., Beyne, E.: Ultra low stress and low temperature patternable silicone materials for applications within microelectronics. *Microelectr. Eng.* **2004**, *76*, 212-218. DOI: 10.1016/j.mee.2004.07.002

[6] Leute, U.: Elektrisch leitfähige Polymerwerkstoffe, *Springer Verlag Essentials*, **2015**, 6-9, DOI: 10.1007/978-3-658-10539-6

[7] Watanabe, M., Sanui, K., Ogata, N., Inoue, F., Kobayashi, T., Ohtaki, Z.: Ionic Conductivity and Mobility of Poly(propylene oxide) Networks Dissolving Alkali Metal Thiocyanates. *Polym. J.* **1985**, *17*, 549-555. DOI: 10.1295/polymj.17.549

[8] Dingels, C., Schömer, M., Frey, H.: Die vielen Gesichter des Poly(ethylenglykols)s, *Chem. Unserer Zeit* **2011**, *45*, 338-349. DOI: 10.1002/ciuz.201100551

[9] Cornet, N., Diat, O., Gebel, G., Jousse, F., Marsacq, D., Mercier, R., Pineri, M.: Sulfonated polyimide membranes: a new type of ion-conducting membrane for electrochemical applications. *J. New Mat. Electrochem. Systems* **2000**, *3*, 33-42. DOI: 10.1021/cm402742u

[10] Cheng, S., Liu, H., Logan, B. L.: Power Densities Using Different Cathode Catalysts (Pt and CoTMPP) and Polymer Binders (Nafion and PTFE) in Single Camber Microbial Fuel Cells. *Environ. Sci. Technol*. **2006**, *40*, 364-369. DOI: 10.1021/es0512071

[11] Saiti, P., Aricó, A. S., Baglio, V., Lufrano, F., Passalacqua, E., Antonucci, V.: Hybrid Nafion-silica membranes doped with heteropolyacids for application in direct methanol fuel cells. *Solid State Ionics* **2001**, *145*, 101-107. DOI: 10.1016/S0167-2738(01)00919-5

[12] Passalacqua, E., Lufrano, F., Squadrito, G., Patti, A., Giorgi, L.: Nafion content in the catalyst layer of polymer electrolyte fuel cells: effects on structure and performance. *Electrochim. Acta* **2001**, *46*, 799-805. DOI: 10.1016/S0013-4686(00)00679-4

[13] Bazuin, C. G., Eisenberg, A.: Ion-Containing Polymers: Ionomers, *J. Chem. Ed*. **1981**, *58*, 938-943. DOI: 10.1021/ed058p938

[14] Zhang, M., Zhang, L., Zhu, M., Wang, Y., Nanwen, L., Zhang, Z., Chen, Q., An, L., Lin, Y., Nan, C.: Controlled functionalization of poly(4-methyl-1-pentene) films for high energy storage applications. *J. Mater. Chem*. A. **2016**, *4*, 4797-4807. DOI: 10.1039/c5ta09949h

[15] U.S. Pat 4351931, E. I. Du Pont de Nemours and Company, Wilmington Del., **1971**.

[16] Wu, K. H., Chang, T. C., Wang, Y. T., Hong, Y. S., Wu, T. S.: Interactions and mobility of copper (II)-imidazole-containing copolymers, *Eur. Polym. J.* **2003**, *39*, 239-245. DOI: 10.1016/S0014-3057(02)00229-X

[17] Tompkins, H. G., Sharma, S. P., The Interaction of Imidazole, Benzimidazole and Related Azoles with a Copper Surface. *Surf. Interf. Anal.* **1982**, *4*, 261-266. DOI: 10.1002/sia.740040609

[18] Prenesti, E., Berto, S.: Interaction of copper(II) with imidazole pyridine nitrogen-containing ligands in aqueous medium: a spectroscopic study. *J. Inorg. Biochem*. **2002**, *88*, 37-43. DOI: 10.1016/S0162-0134(01)00325-7

[19] Jang, J., Jang, I., Kim, H.: Adhesion Promotion of the Polyimide–Copper Interface Using Silane-Modified Polyvinylimidazoles. *J. Appl. Polymer Sci.* **1998**, *68*, 1343-1351. DOI: 10.1002/(SICI)1097-4628(19980523)68

[20] Ding, J., Chen, C., Xue, G.: The Dynamic Mechanical Analysis of Epoxy-Copper Powder Composites Using Azole Compounds as Coupling Agents. *J. Appl. Polym. Sci.* **1991**, *42*, 1459-1464. DOI: 10.1002/app.1991.070420531

[21] Song, S. M., Cho, K., Park, C. E., Yun, H. K., Oh, S. Y.: Synthesis and Characterization of Water-Soluble Polymeric Adhesion Promoter for Epoxy Resin/Copper Joints. *J. Appl. Polym. Sci*. **2002**, *85*, 2202–2210. DOI: 10.1002/app.10837

[22] Lee, K.-W., Walker, G., F., Viehbeck, A.: Formation of polyimide- Cu complexes: improvement of direct Cu-on-PI and PI-on-Cu adhesion. *J. Adh. Sci. Technol.* **1995**, *9*, 1125-1141. DOI: 10.1163/156856195X00941

[23] Boullanger, C., Chapel, J., P., Danel, L., Fournier.: Adhesion Mechanisms of Enamel–Varnishes on Copper: Adhesion Promoter Versus Corrosion Inhibitor*. J. Appl. Polymer Sci*. **2003**, *89*, 952-958. DOI: 10.1002/app.12164

[24] Ines, M., Almeida, G. S., Cattrall, R. W., Kolev, S. D.: Recent trends in extraction and transport of metal ions using polymer inclusion membranes (PIMs). *J. Membr. Sci.* **2012**, *415-416*, 9-23. DOI: 10.1016/j.memsci.2012.06.006

[25] Ulewicz, M., Radzyminska-Lenarcik, E.: Transport of Metal Ions Across Polymer Inclusion Membrane With 1-Alkylimidazole. *Physicochem. Probl. Miner. Process*. **2011**, *46*, 119-130.

[26] Mitiche, L., Tingry, S., Seta, P., Sahmoune, A.: Facilitated transport of copper(II) across supported liquid membrane and polymeric plasticized membrane containing 3-phenyl-4-benzoylisoxazol-5-one as carrier. *J. Membr. Sci.* **2008**, *325*, 605-611. DOI: 10.1016/j.memsci.2008.08.021

[27] Theophanides, T.: Structural and Spectroscopic Properties of Metal-Urea Complexes. *Coord. Chem. Rev.* **1987**, *76*, 237-264. DOI: 10.1016/0010-8545(87)85005-1

[28] Ibrahim, O. B.: Complexes of urea with Mn(II), Fe(III), Co(II), and Cu(II) metal ions. *Adv. Appl. Sci. Res.* **2012**, *3*(6), 3522-3539.

[29] Gangopadhyay, D., Singh, S. K., Sharma, P., Mishra, H., Unnikrishnan, V. K., Singh, B., Singh, R., K.: Spectroscopic and structural study of the newly synthesized heteroligand complex of copper with creatinine and urea. *Spectrochim. Acta A: Mol. Biomol. Spectr.* **2016**, *154*, 200-206. DOI: 10.1016/j.saa.2015.10.028

[30] Jaeger, R. C.: Introduction to Microelectronic Fabrication. Mod. Series Solid State Dev. **2001**, *2,* 18.

[31] Sasago, M., Endo, M., Nakagawa, H., Matsuoka, K., Tani, Y., Hirai, Y., Nomura, N.: New Pattern Transfer Technology For G-line Lithography, *Adv. Resist Technol. Process,* **1989**, *6*, 300-312. DOI:10.1117/12.953042

[32] Stover, H. L., Nagler, M., Bol, I., Miller, V.: Submicron optical lithography: I-line lens and photoresist technology. *Optical Microlithography III: Technology for the Next Decade*, **1984**, *470*, 22-34, DOI:10.1117/12.941878

[33] Okazaki, S.: Resolution limits of optical lithography, *J. Vacuum Sci. Technol. B: Microelectronics Nanometer Struct. Process. Measurement Phenomena*, **1991**, *9*, 2829-2833. DOI:10.1116/1.585650

[34] Sanders, D. P.: Advances in Patterning Materials for 193 nm Immersion Lithography. *Chem. Rev.* **2010**, *110*, 321-360. DOI:10.1021/cr900244n

[35] Jain, K., Willson, C. G., Lin, B. J.: Ultrafast deep UV lithography with excimer lasers, *IEEE Electron Device Letters*, **1982**, *3*, 53-55. DOI:10.1109/EDL.1982.25476

[36] Polasko, K. J., Ehrlich, D. J., Tsao, J. Y., Pease, R. F. W., Marinero, E. E.: Deep UV exposure of Ag2Se/GeSe2 utilizing an excimer laser. *IEEE Electron Device Letters* **1984**, *5*, 24-26. DOI:10.1109/EDL.1984.25818

[37] Uehara, Y., Sasaki, W., Saito, S., Fujiwara, E., Kato, Y., Yamanaka, M. Tsuchida, K., Fujita, J.: High-power argon excimer laser at 126 nm pumped by an electron beam. *Optics Lett.* **1984**, *9*, 539-541. DOI:10.1364/OL.9.000539

[38] Bhaumik, M. L., Bradford Jr, R. S., Ault, E. R.: High-efficiency KrF excimer laser. *Appl. Physics Lett.* **1976**, *28*, 23-24. DOI: org/10.1063/1.88566

[39] Kern, W., The evolution of silicon wafer cleaning technology. *J. Electrochem. Soc.* **1990**, *137*, 1887-1892. DOI: 10.1149/1.2086825

[40] DeSalvo, G. C., Bozada, C. A., Ebel, J. L., Look, D. C., Barrette, J. P., Cerny, C. L., Nakano, K.: Wet chemical digital etching of GaAs at room temperature. *J. Electrochem. Soc.* **1996**, *143*, 3652-3656. DOI: 10.1149/1.1837266

[41] Flamm, D. L., Auciello, O.: Plasma deposition, treatment, and etching of polymers: the treatment and etching of polymers. Elsevier eBook, **2012**. ISBN:9780323139083

[42] Eur. Pat. 0 315 856 B1, Henkel Kommanditgesellschaft auf Aktien, invs.: H.-J. Krause, P. Neumann.

[43] Witte, H., Seeliger, W.; Cyclische Imidsäureester aus Nitrilen und Aminoalkoholen. *Justus Liebigs Ann. Chem* **1974**, 996–1009. DOI: 10.1002/jlac.197419740615.

[44] Tomalia, A. D., Sheetz, D. P.: Homopolymerization of 2-Alkyl- and 2-Aryl-2-Oxazolines. *J. Polym. Sci. A* **1966**, *4*, 2253-2265. DOI: 10.1002/pol.1966.150040919

[45] Seeliger, W., Aufderhaar, E., Diepers, W., Feinauer, E., Nehring, R., Thier, W., Hellmann, H.: Recent Syntheses and Reactions of Cyclic Imidic Esters, *Angew. Chem. Internat. Ed.* **1966**, *5*, 875-888, DOI: 10.1002/anie.196608751

[46] Lew, P., Krutzik, P. O., Hart, M. E., Chamberlin, A.R.: Increasing Rates of Reaction: Microwave-Assisted Organic Synthesis for Combinatorial Chemistry. *J. Comb. Che.* **2002**, *4*, 95-105. DOI: 10.1021/cc010048o

[47] Kappe, C. O.: Controlled Microwave Heating in Modern OrganicSynthesis. A*ngew. Chem. Int. Ed.* **2004**, *43*, 6250-6284, DOI: 10.1002/anie.200400655

[48] Bilecka, I., Niederberger, M.: Microwave chemistry for inorganic nanomaterials synthesis. *Royal Society of Chemistry* **2010**, *2*, 1358-1374. DOI: 10.1039/b9nr00377k

[49] Wiesbrock, F., Hoogenboom, R., Schubert, U. S: Microwave-Assisted Polymer Synthesis:State-of-the-Art and Future Perspectives. *Macromol. Rapid Commun.* **2004**, *25*, 1739-1764, DOI: 10.1002/marc.200400313

[50] Wiesbrock, F., Hoogenboom, R., Leenen, M. A. M., Meier, M. A. R., Schubert, U. S.: Investigation of the Living Cationic Ring-Opening Polymerization of 2-Methyl-, 2-Ethyl-, 2-Nonyl-, and 2-Phenyl-2-oxazoline in a Single-Mode Microwave Reactor. *Macromolecules* **2005**, *38*, 5025-5034. DOI: 10.1021/ma0474170

[51] Wiesbrock, F., Hoogenboom, R., Abeln, C. H., Schubert, U. S.: Single-Mode Microwave Ovens as New Reaction Devices: Accelerating the Living Polymerization of 2-Ethyl-2-Oxazoline. *Macromol. Rapid Commun*. **2004**, *25*, 1895-1899. DOI: 10.1002/marc.200400369

[52] Hoogenboom, R., Wiesbrock, F., Huang, H., Leenen, M. A M., Thijs, H. M. L., van Nispen, S. F. G. M., van der Loop, M., Fustin, C.-A., Jonas, A. M., Gohy, J.-F., Schubert, U. S.: Microwave-Assisted Cationic Ring-Opening Polymerization of 2-Oxazolines: A Powerful Method for the Synthesis of Amphiphilic Triblock Copolymers, *Macromolecules* **2006**, *39*, 4719-4725, DOI: 10.1021/ma060952a

[53] Hallensleben, M. L., Fuss, R., Mummy. F.: Polyvinyl Compounds, Others, *Ullmann's Encyclopedia of Industrial Chemistry* **2015**. DOI: 10.1002/14356007.a21_743.pub2

[54] Kolb, H. C., Finn, M. G., Sharpless, K. B.: Click Chemistry: Diverse Chemical Function from a Few Good Reactions. *Angew. Chem. Int. Ed*. **2001**, *40*, 2004-2021. DOI: 10.1002/1521-3773(20010601)40:11<2004::AID-ANIE2004>3.0.CO;2-5

[55] Hoyle, C. E., Bowman, C. N.: Thiol-En-Klickchemie, *Angew. Chem.* **2010**, *122*, 1584-1617. DOI: 10.1002/ange.200903924

[56] Cook, W. D., Chen, F., Pattison, D. W., Hopson, P., Beaujon, M.: Thermal polymerization of thiol-ene network-forming systems. *Polym Int*. **2007**, *56*, 1572-1579. DOI: 10.1002/pi.2314

[57] Xu, J., Boyer, C., Visible Light Photocatalytic Thiol−Ene Reaction: An Elegant Approach for Fast Polymer Postfunctionalization and Step-Growth Polymerization. *Macromolecules* **2015**, *48*, 520-529. DOI: 10.1021/ma502460t

[58] Campos, L. M., Killiops, K. L., Sakai, R., Paulusse, J. M. J., Daniron, D., Drockenmuller, E., Messmore, B. W., Hawker, C. J.: Development of Thermal and Photochemical Strategies for Thiol-Ene Click Polymer Functionalization. *Macromolecules* **2008**, *41*, 7063-7070, DOI: 10.1021/ma801630n

[59] Kempe, K., Hoogenboom, R.; Schubert, U. S.: A green approach for the synthesis and thiol-ene modification of alkene functionalized poly(2-oxazoline)s. *Macromol. Rapid Commun*. **2011**, *32*, 1484-1489, DOI: 10.1002/marc.201100271

[60] Schlenk, V., Ellmaier, L., Rossegger, E., Edler, M., Griesser, T., Weidinger, G., Wiesbrock, F.: Water-Developable Poly(2-oxazoline)-Based Negative Photoresists. *Macromol. Rapid Commun.* **2012**, *33*, 396-340. DOI: 10.1002/marc.201100717

[61] Yaroshchuk, A., Luxbacher, T.: Electrokinetics in undeveloped flows, *J. Colloid Interf. Sci.* **2013**, *410*, 195-201.DOI: 10.1016/j.jcis.2013.08.021

[62] Hoeppener, S., Wiesbrock, F., Hoogenboom, R., Thijs, H. M. L., Schubert, U. S.: Morphologies of Spin-Coated Films of a Library of Diblock Copoly(2-oxazoline)s and Their Correlation to the Corresponding Surface Energies. *Macromol. Rapid Commun.* **2006**, *27*, 405-411. DOI: 10.1002/marc.200500863